Progress in Oceanography 213 (2023) 102998

Contents lists available at ScienceDirect

Progress in Oceanography

journal homepage: www.elsevier.com/locate/pocean

Body size, depth of occurrence, and local oceanography shape trophic structure in a diverse deep-pelagic micronekton assemblage

Travis M. Richards [a,*], Tracey T. Sutton [b], Matthew S. Woodstock [c], Heather Judkins [d], R.J. David Wells [a,e]

[a] Department of Marine Biology, Texas A&M University at Galveston, Galveston, TX, United States
[b] Guy Harvey Oceanographic Center, Halmos College of Arts and Sciences, Nova Southeastern University, Dania Beach, FL, United States
[c] Department of Biological Sciences, Oceans and Coastal Division, Institute of Environment, Florida International University, Miami, FL, United States
[d] Integrative Biology, University of South Florida St. Petersburg, St. Petersburg, FL, United States
[e] Department of Ecology & Conservation Biology, Texas A&M University, College Station, TX, United States

ARTICLE INFO

Keywords:
Mesopelagic
Bathypelagic
Gulf of Mexico
Food webs
Stable isotope analysis
Trophic structure
Diet

ABSTRACT

The Gulf of Mexico's (GOM) deep-pelagic realm is one of the planet's most speciose pelagic ecoregions, but detailed knowledge of ecosystem structure and function is lacking. Understanding trophic structure is critical to understanding ecosystem dynamics as trophic interactions regulate the flow of energy through ecosystems and influence the resilience of ecosystems to disturbance. Using novel stable isotope (SIA) data and historical stomach content (SCA) data, we examined deep-pelagic trophic structure using 58 species of micronekton from the GOM that encompassed a variety of migratory behaviors, depth distributions, and trophic strategies. We identified major trophic groupings, explored the extent that differences in diet, body size, vertical migration, and presence of a mesoscale feature (Loop Current) explained micronekton isotopic variation and estimated species-specific trophic positions. Cluster analysis of SIA data identified four trophic groups, although species were not strictly clustered by diet. Specifically, non-migratory zooplanktivores with elevated $\delta^{15}N$ values were grouped with vertically migrating piscivores, suggesting some non-migratory species could be feeding within food chains with elevated isotopic baselines. The mean $\delta^{13}C$ values of species encompassed a narrow range from −21.6 ‰ to −18.1 ‰, with variation in $\delta^{13}C$ values of vertically migrating species explained by a positive relationship with body size and higher $\delta^{13}C$ values in Loop Current water. In contrast, variation in $\delta^{13}C$ values of non-migrators was primarily explained by elevated values in deeper-dwelling species and in larger species. The mean $\delta^{15}N$ values of species ranged between 5.0 ‰ and 11.5 ‰, with variation in $\delta^{15}N$ values of vertical migrators explained by a positive relationship with body size and lower $\delta^{15}N$ values in Loop Current water. Variation in the $\delta^{15}N$ values of non-migrators was largely explained by elevated $\delta^{15}N$ values in deeper-dwelling species and in larger-bodied species. Trophic position (TP) estimations for the assemblage ranged between 2.6 and 4.9. The elevated $\delta^{15}N$ values in non-migratory species led to higher TP estimates relative to estimates derived from stomach content data, but agreement between TP estimates using SIA and SCA was high for vertically migrating taxa. This discrepancy may be a factor of vertical migrating species having a more similar feeding depth than non-migrators. Our results provide important insight into the trophic organization of low-latitude oligotrophic ecosystems and demonstrate that trophic variation within micronekton assemblages is primarily driven by differences in body size, location in the water column and position relative to salient oceanographic features.

1. Introduction

The deep-pelagic ocean (water column seaward of the continental shelf; greater than 200-m depth) is the largest and least studied marine ecosystem on the planet (Webb et al., 2010). Encompassing greater than 90 % of the world's living space by volume, the deep-pelagic realm affects all life on Earth through its vital roles in the global carbon and climate cycles (Mengerink et al., 2014; Thurber et al., 2014). Despite their vast size, deep-pelagic ecosystems are changing due to climate change, ocean acidification, overfishing, and natural resource extraction

* Corresponding author.
E-mail address: trichar3@ucsc.edu (T.M. Richards).

https://doi.org/10.1016/j.pocean.2023.102998
Received 18 May 2022; Received in revised form 31 January 2023; Accepted 20 February 2023
Available online 24 February 2023

(Ramirez-Llodra et al., 2011; Drazen et al., 2020; Murawski et al., 2020). Considering the persistent stressors affecting the deep pelagial and their potential to change ecosystem structure and function, there has been a concerted effort to better understand and describe deep-pelagic ecosystem dynamics so that management plans can be created and implemented (Ramirez-Llodra et al., 2011; Drazen et al., 2020).

A thorough understanding of trophic structure is critical to understanding deep-pelagic ecosystem function as trophic dynamics determine the flow of energy through ecosystems. Micronekton, small (2–10 cm) fishes, crustaceans, and cephalopods, are numerically dominant components of deep-pelagic communities and critical to delineating trophic structure and energy pathways in deep-pelagic ecosystems (Irigoien et al., 2014; Choy et al., 2016; Vereshchaka et al., 2019). Due in part to their high global abundance, micronekton are ecologically important as both predators and prey (Hopkins et al., 1996; Choy et al., 2013; Young et al., 2015; Drazen and Sutton, 2017). As predators, micronekton are important consumers of zooplankton (Hopkins and Gartner, 1992; Drazen and Sutton, 2017) and, as prey, are important contributors to the diets of marine mammals, seabirds, and economically valuable fishes, including tunas and billfishes (Pauly et al., 1998; Moteki et al., 2001; Cherel et al., 2010; Choy et al., 2013). Many deep-pelagic micronekton species undertake diel vertical migrations (DVM) at night from *meso-* and sometimes bathypelagic depths to access the food-rich waters of the epipelagic zone, while remaining hidden from visually cued predators before returning to depth at dawn (Pearre Jr., 2003; Brierly, 2014; Behrenfeld et al., 2019). Through DVM, micronekton actively transport surface-derived primary production to deep-pelagic communities by excretion of waste and calcium carbonate, respiration of CO_2, and their own consumption by predators at depth (Sutton and Hopkins, 1996a; Davison et al., 2013; Trueman et al., 2014; Saba et al., 2021).

Trophic structure in marine systems is typically investigated using stomach content analysis (SCA) and stable isotope analysis (SIA). The two methods are complimentary as SCA provides direct evidence of feeding relationships among species (Hyslop, 1980; Winemiller and Polis, 1996), while SIA provides a broader view of trophic structure and can be used to trace the flow of energy from primary producers to higher-order consumers (Peterson and Fry, 1987; Vander Zanden and Rasmussen, 2001). Additionally, the two methods integrate feeding information over differing timescales, with SCA providing an estimate of diet over timescales relative to digestion rates (hours to days), while SIA integrates feeding information over timescales relative to tissue turnover rates (weeks to months; Hyslop, 1980; Hesslein et al., 1993; MacAvoy et al., 2001; Sakano et al., 2005). The $\delta^{13}C$ values of consumer tissues undergo minimal trophic fractionation (from ~ 0.5 to 1 ‰) but can vary markedly between primary producers with differing photosynthetic pathways (Peterson and Fry, 1987), which can be used to estimate the relative contributions of carbon sources or habitats contributing to consumer production (DeNiro and Epstein, 1978; Wada et al., 1991). In contrast, $\delta^{15}N$ values of consumer tissues undergo predictable enrichment at each trophic level (from 2 to 4 ‰ per trophic level; Minagawa and Wada, 1984; Caut et al., 2009) and are used to estimate trophic position and food chain length (Minagawa and Wada, 1984; Post, 2002; Hussey et al., 2014).

The Gulf of Mexico (GOM) is a semi-enclosed ocean basin and marginal sea of the greater Atlantic Ocean and with a deep-pelagic faunal assemblage that is considered transitional between the subtropical North Atlantic and Caribbean Sea (Bangma and Haedrich, 2008). With recent pelagic faunal inventories identifying 897 fish species, 120 species of crustaceans, and 94 species of cephalopod, the micronekton assemblage in the pelagic GOM is considered one of the World Ocean's most speciose pelagic ecoregions (Sutton et al., 2017a; Sutton et al., 2020). In addition to a diverse pelagic fauna, the GOM supports lucrative coastal and pelagic fisheries and is the focus of intense oil and gas exploration and extraction that has steadily expanded into deeper water (Murawski et al., 2020). Despite the deep-pelagic GOM's standing with respect to global oceanic biodiversity and its regional importance to local economies, detailed knowledge of trophic structure and ecosystem functioning in the pelagic GOM is incomplete, as it is for the overwhelming majority of the oceanic domain. Through the combined use of stable isotope analysis and historical stomach content data from oceanic micronekton from the GOM, we will: 1) delineate major trophic groups using SIA data and compare SIA trophic groupings with previous trophic group estimations made using SCA; 2) use multiple linear regression to model isotopic variation in the micronekton assemblage to examine how differences in diet, body size, vertical migration, and spatial distribution influence trophic structure; and 3) provide trophic position estimates for each micronekton species with a comparison between estimations made using SIA and SCA data.

2. Methods

2.1. Sample collection and study design

Micronekton samples were collected from August 2015 to August 2016 during three oceanographic cruises in the northern GOM as part of the Gulf of Mexico Research Initiative (GOMRI)-funded Deep Pelagic Nekton Dynamics of the Gulf of Mexico (DEEPEND) program (Milligan et al., 2018; Cook et al., 2020; Sutton et al. 2020). Sampling stations visited during cruises were located within the same region of the GOM (Fig. 1) but varied by cruise according to the changing position of the Loop Current, which was targeted during DEEPEND sampling (Johnston et al., 2019; Cook et al., 2020). Large-scale circulation within the northern GOM is dominated by the Loop Current (Vukovich and Crissman, 1986; Davis et al., 2002), with concomitant effects on the distributions of primary production, zooplankton, and nekton (Davis et al., 2002; Rooker et al., 2013). Because stable isotope ratios of micronekton can vary across mesoscale oceanographic features in the GOM (Wells et al., 2017; Richards et al., 2020), sampling stations during each cruise were identified as either Gulf Common Water (GCW) or Loop Current water (LCW) following Johnston et al. (2019), with some sampling sites identified as GCW and LCW on different cruises (Fig. 1). Micronekton were collected using a 10-m^2 multiple opening and closing net with environmental sensing system (MOCNESS, hereafter), which consisted of six nets constructed of 3-mm nylon mesh and PVC codends. During sampling, the individual nets of the MOCNESS were opened and closed at discrete depths in the epipelagic (0–200 m), upper-mesopelagic (200–600 m), lower-mesopelagic (600–1000 m), and upper bathypelagic (1000–1200 m & 1200–1500 m) zones, with the first net fished from 0 to 1500-m obliquely (Cook et al., 2020). Upon retrieval of the MOCNESS, micronekton were sorted, identified to species, and enumerated. Samples for SIA were frozen whole at −20ºC until processing at Texas A&M University at Galveston.

Species were selected for SIA analysis based on their abundance, migratory behavior (vertical migrators vs non-migrators), depth distributions, and trophic guilds (detritivores, zooplanktivores, micronektivores, piscivores) to provide a comprehensive view of trophic structure (Table 1). Additionally, species included in previous diet studies of deep-pelagic micronekton in the GOM (e.g., Passarella and Hopkins, 1991; Hopkins et al., 1996; Sutton and Hopkins, 1996a; Burghart et al., 2010) were purposefully selected to allow for comparisons between descriptions of trophic structure derived from SCA and SIA. Samples of highly abundant species were haphazardly collected across as many sampling stations as possible to incorporate population-level variation, while rarer species were sampled opportunistically.

2.2. Stable isotope analysis

Samples for SIA were dissected from the lateral musculature of fishes, the anterior mantle of cephalopods, and the abdomen of crustaceans (Bunn et al., 1995; Pinnegar & Polunin, 1999). Following dissection, all samples were cleaned of skin, scales, bones, or

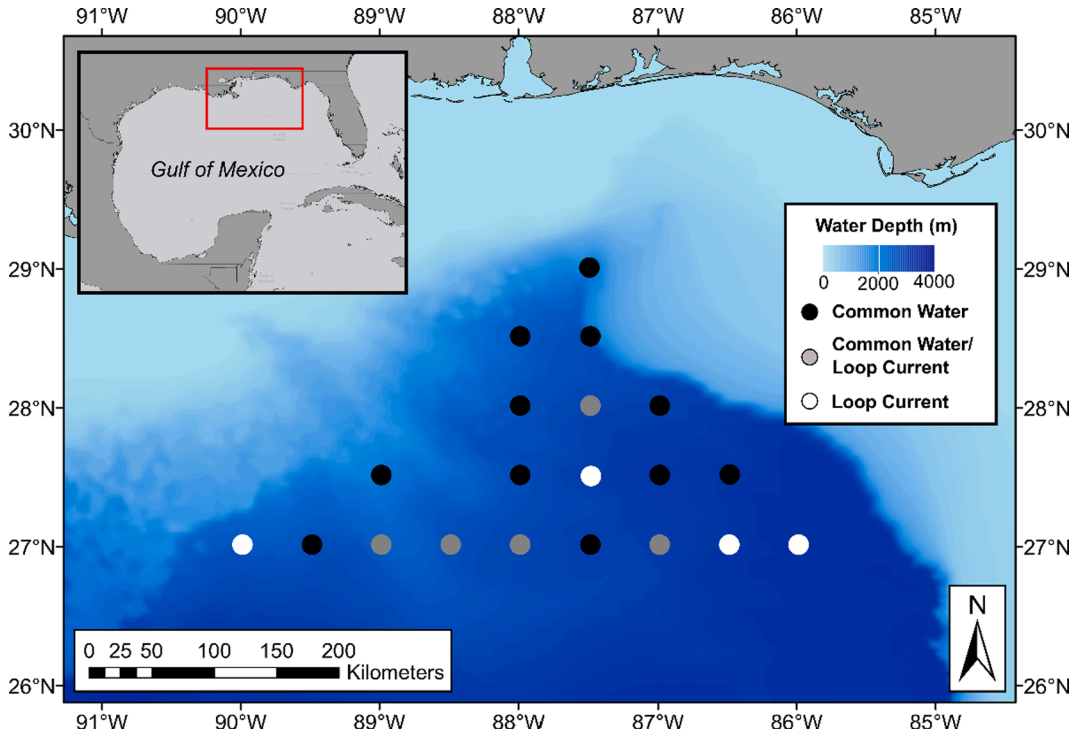

Fig. 1. Map of the northern Gulf of Mexico showing collection locations for micronekton analyzed for stable isotope analysis. Black circles represent locations occupied by Gulf Common Water at the time of collections, white circles represent locations occupied by Loop Current Water, and grey circles represent collection locations occupied by Gulf Common and Loop Current water on different cruises.

exoskeleton and rinsed with deionized water to remove any trace carbonates (Schlacher & Connolly, 2014). All isotope samples were then freeze dried and homogenized using an agate mortar and pestle. Following homogenization, ~0.8 mg of sample was transferred by hand to tin capsules (3x5 mm) that were then sealed before shipment to the UC Davis Stable Isotope Facility. Samples were analyzed for $\delta^{13}C$ and $\delta^{15}N$ isotopes using a PDZ Europa ANCA-GSL elemental analyzer coupled with a PDZ Europa 20–20 isotope ratio mass spectrometer. Stable isotope data are expressed in δ-notation as the deviation from the international standards Vienna PeeDee belemnite and atmospheric N_2 for carbon and nitrogen, respectively. The UC Davis Stable Isotope Facility reports a long-term standard deviation of 0.2 ‰ for $\delta^{13}C$ and 0.3 ‰ for $\delta^{15}N$. All stable isotope values are reported in δ notation, measured as parts per thousand differences from an international standard (‰) according to equation (1).

$$\delta x = \left(\frac{R_{sample}}{R_{standard}} - 1\right) x1000 \quad (1)$$

Where × represents the isotope of C or N and *R* represents the ratio of heavy to light isotope in the element (i.e. ^{13}C:^{12}C or ^{15}N:^{14}N). Mean C:N values of micronekton species ranged between 3.18 and 4.40, suggesting lipid content in samples could confound the interpretation of $\delta^{13}C$ values (Post, 2007). Thus, all $\delta^{13}C$ values were mathematically corrected according to Post et al. (2007) before statistical analyses were performed.

2.3. Trophic position designations

Trophic position estimates using SIA (TP:SIA) were made using equation (2).

$$TrP_i = \left(\delta^{15}N_i - \delta^{15}N_{Base}\right)/\Delta^{15}N + \lambda \quad (2)$$

where $\delta^{15}N_i$ is the nitrogen isotopic signature of an individual belonging to species i, $\delta^{15}N_{Base}$ is the nitrogen isotopic signature of the primary producer or consumer used to set the baseline, $\Delta^{15}N$ is the expected level of $\delta^{15}N$ fractionation between predator and prey (Post, 2002), and λ represents the trophic level of the baseline organism (2 for primary consumer). Due to the absence of trophic discrimination factors (TDFs) for deep-pelagic taxa, TDFs derived from laboratory experiments of shallower-dwelling marine fishes ($\Delta^{15}N = 3.15$; Sweeting et al., 2007), and crustaceans (mean $\Delta^{15}N = 2.50$; Parker et al., 1989; Dittel et al., 1997; Vanderklift and Ponsard, 2003; Downs et al., 2014) were employed. Due to a lack of cephalopod specific TDFs in the primary literature, the TDF for fishes outlined by Sweeting et al. (2007) was applied to cephalopods. Samples of the tunicate *Pyrosoma atlanticum* (n = 12) collected concurrently with micronekton were used to set the nitrogen isotopic baseline ($\delta^{15}N_{Base}$ in Equation (2)). Pyrosomes feed on suspended organic matter throughout the water column and represent the primary consumer trophic position in low-latitude oligotrophic ecosystems, such as the pelagic GOM. In these ecosystems, phytoplankton communities primarily comprise small flagellates rather than large diatoms, which are unassimilated during pyrosome feeding (Harbou et al., 2011; Pakhomov et al., 2019). The $\delta^{15}N$ values of *P. atlanticum* (range: 2.5–3.9 ‰; mean ± s.d: 3.11 ± 0.44) collected during the study were consistent with median $\delta^{15}N$ values of epipelagic copepods (a dominant food source of migratory deep-pelagic fishes) and other epipelagic zooplankton reported from the GOM (range: 1–5 ‰; Holl et al., 2007; Wells et al., 2017) and greater Atlantic Ocean (range: 0–6 ‰; Montoya et al., 2002; Nolé Eduardo et al., 2020). Pyrosome isotopic values were averaged across stations and mesoscale features due to the observation of similar isotopic values across the sampling area, and the ability of pyrosomes as primary consumers to integrate isotopic baselines across vertical and horizontal spatial scales.

Our trophic position estimates from SIA (TP:SIA) were compared to estimates derived from historical stomach content data (TP:SCA) to determine concordance in the two methods. Estimates of TP:SCA for fishes were taken from FishBase.org, while estimates for crustaceans and cephalopods, were taken from SeaLifeBase.org (Palomares and Pauly, 2021). Estimates of TP:SCA derived from a single prey item in FishBase and SeaLifeBase were excluded from this analysis. For a detailed

Table 1
Summary table depicting sample sizes, length, $\delta^{13}C$, $\delta^{15}N$ values (mean ± SD), median day and nighttime depth of occurrence, and trophic position estimates for micronekton analyzed for stable isotope analysis. *n*: number of samples; M/NM: M, migrator; NM, non-migrator; TP:SCA: trophic position derived from historical stomach content data in the primary literature; TP:SIA: trophic position estimates made using stable isotope analysis.

Family	Species	*n*	M/NM	Body Length (mm)	$\delta^{13}C$ (‰)	$\delta^{15}N$ (‰)	Med. Night Depth (m)	Med. Day Depth (m)	Diet Guild	TP: SCA	TP: SIA
Fishes											
Anoplogastridae	*Anoplogaster cornuta*	4	NM	124.3 ± 8.1	−19.1 ± 0.3	9.9 ± 1.1	628	950	Pisc.	4.0	4.2 ± 0.3
Ariommatidae	*Ariomma bondi*	3	NM	63.7 ± 4.2	−19.3 ± 0.1	6.6 ± 0.2	100	100	–	–	3.1 ± 0.1
Bathylagidae	*Dolicholagus longirostris*	5	M	106.0 ± 26.6	−19.9 ± 0.5	7.5 ± 0.7	175	960	Zoop 6	3.4	3.4 ± 0.2
Congridae	*Rhynchoconger flavus*	5	NM	43.0 ± 7.9	−21.6 ± 0.4	5.5 ± 0.4	100	100	Detr.	–	2.8 ± 0.1
Gonostomatidae	*Cyclothone acclinidens*	10	NM	31.8 ± 3.0	−18.3 ± 0.3	10.5 ± 0.5	850	850	Zoop 1	3.5	4.4 ± 0.2
Gonostomatidae	*Cyclothone alba*	10	NM	25.8 ± 1.7	−19.6 ± 0.3	7.5 ± 0.5	425	425	Zoop 1	3.1	3.4 ± 0.2
Gonostomatidae	*Cyclothone braueri*	10	NM	23.4 ± 1.4	−19.1 ± 0.3	6.9 ± 0.5	500	500	Zoop 1	3.1	3.2 ± 0.2
Gonostomatidae	*Cyclothone obscura*	20	NM	44.0 ± 5.7	−18.4 ± 0.4	10.5 ± 0.9	1950	1950	Zoop 1	3.1	4.3 ± 0.3
Gonostomatidae	*Cyclothone pallida*	10	NM	42.9 ± 6.6	−18.7 ± 0.7	9.6 ± 0.9	850	850	Zoop 1	3.2	4.1 ± 0.3
Gonostomatidae	*Cyclothone pseudopallida*	10	NM	33.2 ± 4.2	−19.4 ± 0.3	8.2 ± 0.3	650	600	Zoop 1	3.1	3.6 ± 0.1
Gonostomatidae	*Sigmops elongatus*	20	M	102.8 ± 32.9	−19.1 ± 0.4	8.8 ± 0.6	175	575	Zoop 2	3.3	3.8 ± 0.2
Melamphaidae	*Melamphaes simus*	19	M	22.4 ± 3.9	−19.4 ± 0.5	9.0 ± 1.1	600	850	Zoop 1	–	3.9 ± 0.4
Melamphaidae	*Poromitra gibbsi*	3	NM	103.5 ± 12.0	−19.2 ± 0.4	10.9 ± 0.4	800	900	Gelat.	3.7	4.5 ± 0.1
Melamphaidae	*Scopeloberyx opercularis*	7	NM	26.3 ± 1.1	−18.9 ± 0.2	11.1 ± 0.4	1050	1050	Zoop 1	3.1	4.6 ± 0.1
Melamphaidae	*Scopeloberyx opisthopterus*	5	NM	22.8 ± 1.9	−20.0 ± 0.4	9.3 ± 1.0	900	1050	Zoop 1	–	4.0 ± 0.3
Melamphaidae	*Scopeloberyx robustus*	4	NM	19.8 ± 1.5	−19.8 ± 0.7	8.8 ± 0.9	1050	1050	Zoop 1	–	3.9 ± 0.3
Myctophidae	*Benthosema suborbitale*	16	M	25.9 ± 3.6	−19.3 ± 0.3	8.2 ± 0.9	80	500	Zoop 1	3.4	3.6 ± 0.3
Myctophidae	*Bolinichthys photothorax*	7	M	31.0 ± 10.2	−19.5 ± 0.3	7.5 ± 0.7	150	625	Zoop 1	–	3.4 ± 0.2
Myctophidae	*Centrobranchus nigroocellatus*	2	M	38.0 ± 0.0	−20.4 ± 0.1	5.0 ± 0.7	75	475	Zoop 7	3.4	2.6 ± 0.2
Myctophidae	*Ceratoscopelus warmingii*	8	M	39.5 ± 16.2	−19.7 ± 0.5	7.4 ± 1.0	100	825	Zoop 2	3.4	3.4 ± 0.3
Myctophidae	*Diaphus dumerilii*	8	M	36.8 ± 7.8	−19.5 ± 0.4	8.4 ± 0.6	105	450	Zoop 1	–	3.7 ± 0.2
Myctophidae	*Diaphus lucidus*	10	M	51.8 ± 17.1	−19.8 ± 0.6	8.9 ± 0.8	180	725	Zoop 3	–	3.8 ± 0.3
Myctophidae	*Diaphus mollis*	10	M	36.6 ± 7.8	−19.6 ± 0.3	9.1 ± 0.7	138	650	Zoop 1	–	3.9 ± 0.2
Myctophidae	*Diaphus splendidus*	5	M	35.0 ± 17.7	−19.5 ± 0.3	8.1 ± 1.1	140	450	Zoop 1	–	3.6 ± 0.4
Myctophidae	*Diogenichthys atlanticus*	4	M	17.8 ± 1.8	−20.6 ± 0.2	6.8 ± 0.4	135	525	Zoop 1	3.1	3.2 ± 0.1
Myctophidae	*Hygophum benoiti*	4	M	18.3 ± 1.0	−19.0 ± 0.5	7.8 ± 0.9	125	500	Zoop 1	–	3.5 ± 0.3
Myctophidae	*Hygophum taaningi*	8	M	29.4 ± 6.5	−19.0 ± 0.3	8.0 ± 0.9	155	675	Zoop 1	3.2	3.6 ± 0.3
Myctophidae	*Lampadena luminosa*	8	M	22.6 ± 4.7	−19.3 ± 0.5	6.1 ± 0.7	208	750	Zoop 5	–	3.0 ± 0.2
Myctophidae	*Lampanyctus alatus*	16	M	36.0 ± 7.9	−19.5 ± 0.5	8.0 ± 0.7	115	625	Zoop 2	3.2	3.5 ± 0.2
Myctophidae	*Lepidophanes guentheri*	21	M	34.2 ± 11.0	−18.9 ± 0.6	6.9 ± 1.2	115	650	Zoop 2	3.1	3.2 ± 0.4
Myctophidae	*Myctophum affine*	10	M	31.0 ± 10.5	−19.4 ± 0.6	8.4 ± 1.2	78	500	Zoop 1	–	3.7 ± 0.4
Myctophidae	*Nannobrachium lineatum*	9	M	87.3 ± 7.3	−19.3 ± 0.2	8.7 ± 0.5	500	900	Zoop 2	–	3.8 ± 0.2
Myctophidae	*Notolychnus valdiviae*	10	M	18.4 ± 1.9	−19.9 ± 0.3	7.3 ± 0.7	105	450	Zoop 1	3.1	3.3 ± 0.2
Myctophidae	*Notoscopelus resplendens*	4	M	33.8 ± 12.1	−19.8 ± 0.4	7.5 ± 1.6	138	1050	Zoop 2	–	3.4 ± 0.5
Phosichthyidae	*Pollichthys mauli*	5	M	34.6 ± 7.4	−19.1 ± 0.2	7.5 ± 0.9	100	400	Zoop 2	3.7	3.4 ± 0.3

(*continued on next page*)

Table 1 (*continued*)

Family	Species	*n*	M/NM	Body Length (mm)	$\delta^{13}C$ (‰)	$\delta^{15}N$ (‰)	Med. Night Depth (m)	Med. Day Depth (m)	Diet Guild	TP: SCA	TP: SIA
Phosichthyidae	*Vinciguerria nimbaria*	5	M	27.8 ± 6.8	−19.1 ± 0.3	7.8 ± 0.6	100	400	Zoop 1	3.1	3.5 ± 0.2
Sternoptychidae	*Argyropelecus aculeatus*	4	M	36.8 ± 11.3	−19.4 ± 0.3	8.3 ± 0.3	213	325	Zoop 3	3.7	3.6 ± 0.1
Sternoptychidae	*Argyropelecus hemigymnus*	15	NM	26.1 ± 4.1	−18.8 ± 0.4	9.1 ± 0.6	325	363	Zoop 4	3.1	3.9 ± 0.2
Sternoptychidae	*Sternoptyx diaphana*	13	NM	22.8 ± 6.4	−19.6 ± 0.2	8.6 ± 0.7	650	750	Zoop 5	3.2	3.7 ± 0.2
Sternoptychidae	*Sternoptyx pseudobscura*	17	NM	28.3 ± 9.3	−19.7 ± 0.3	8.1 ± 0.4	850	900	Zoop 2	3.4	3.6 ± 0.1
Sternoptychidae	*Valenciennellus tripunctulatus*	5	NM	24.2 ± 1.3	−19.8 ± 0.2	9.0 ± 0.4	340	400	Zoop 1	3.1	3.9 ± 0.1
Stomiidae	*Chauliodus sloani*	11	M	179.9 ± 39.6	−18.6 ± 0.3	9.0 ± 0.6	463	575	Pisc.	4.3	3.9 ± 0.2
Stomiidae	*Echiostoma barbatum*	4	M	234.3 ± 35.0	−18.1 ± 0.6	9.9 ± 0.5	500	1250	Pisc.	4.1	4.2 ± 0.2
Stomiidae	*Photostomias guernei*	5	M	83.8 ± 25.4	−18.7 ± 0.5	8.7 ± 0.3	500	750	Micro.	3.5	3.8 ± 0.1
Stomiidae	*Stomias affinis*	5	M	136.6 ± 16.8	−18.6 ± 0.5	9.7 ± 0.7	450	650	Pisc.	4.3	4.1 ± 0.2
Crustaceans											
Eucopiidae	*Eucopia sculpticauda*	4	NM	39.5 ± 1.3	−18.9 ± 0.3	10.4 ± 0.4	1650	1550	Zoop 1	–	4.9 ± 0.2
Euphausiidae	*Thysanopoda acutifrons*	5	M	33.8 ± 2.2	−19.3 ± 0.1	9.1 ± 0.5	750	750	Zoop 1	3.7	4.4 ± 0.2
Oplophoridae	*Acanthephyra curtirostris*	13	NM	65.3 ± 27.1	−18.5 ± 0.2	9.1 ± 0.5	850	1050	Micro.	3.8	4.4 ± 0.2
Oplophoridae	*Acanthephyra purpurea*	10	M	62.0 ± 12.7	−18.2 ± 0.5	7.6 ± 0.5	175	850	Zoop 2	–	3.8 ± 0.2
Oplophoridae	*Acanthephyra stylorostratis*	6	NM	40.5 ± 6.9	−18.7 ± 0.2	9.0 ± 0.4	1050	1050	Micro.	4.0	4.3 ± 0.1
Oplophoridae	*Systellaspis debilis*	6	M	40.5 ± 7.7	−18.8 ± 0.6	7.2 ± 0.7	175	675	Zoop 2	3.5	3.6 ± 0.3
Sergestidae	*Gardinerosergia splendens*	11	M	35.3 ± 3.4	−19.6 ± 0.5	6.7 ± 0.7	275	725	Zoop 2	3.6	3.4 ± 0.3
Cephalopods											
Amphitretidae	*Bolitaena pygmaea*	3	NM	10.5 ± 0.8	−19.1 ± 0.4	7.0 ± 1.2	600	600	Zoop 1	3.7	3.2 ± 0.4
Amphitretidae	*Japetella diaphana*	5	NM	22.5 ± 11.5	−19.2 ± 0.5	6.6 ± 1.1	750	750	Zoop 1	3.6	3.1 ± 0.3
Histioteuthidae	*Stigmatoteuthis arcturi*	4	M	9.5 ± 2.1	−19.7 ± 0.2	9.5 ± 0.7	600	750	Zoop 1	–	4.0 ± 0.2
Mastigoteuthidae	*Mastigoteuthis agassizii*	2	NM	68.5 ± 3.5	−18.3 ± 0.1	11.5 ± 0.8	750	850	Pisc.	–	4.7 ± 0.2
Pyroteuthidae	*Pterygioteuthis gemmata*	6	M	11.0 ± 4.1	−19.5 ± 0.3	8.0 ± 0.3	300	750	Zoop 1	–	3.6 ± 0.1
Vampyroteuthidae	*Vampyroteuthis infernalis*	3	NM	14.0 ± 6.9	−19.0 ± 0.2	10.4 ± 2.3	1300	1300	Zoop 1	3.5	4.3 ± 0.7

description of the methods used by FishBase and SeaLifeBase to calculate TP we refer the reader to Mancinelli et al. (2013) and Froese and Pauly (2010).

2.4. Feeding guild determination

To allow for comparisons between trophic structure characterizations using our SIA data and historical SCA data, we used criteria identified by Hopkins et al. (1996) in their diet analysis of 164 species of deep-pelagic fishes in the GOM to assign micronekton species to feeding guilds (Czudaj et al., 2020). For crustaceans, cephalopods, and fishes not included in Hopkins et al. (1996), diet data were taken from primary literature sources and applied to the same feeding guild criteria. To allow for the identification of ontogenetic diet shifts, Hopkins et al. (1996) divided individuals from each species into 10-mm size classes, which were used as the base unit in cluster analyses (as opposed to species). This method resulted in some species having differing size classes assigned to different feeding guilds. For species represented by multiple feeding guilds, we calculated the mean size of individuals included in our analysis and assigned all individuals of the species to the corresponding feeding guild. A description of the feeding guilds represented by the species examined in this study is given in Table 2. The references from the primary literature used to assign species in this study to feeding guilds can be viewed in Supplemental Table S1. Although the diet data used to assign species to feeding guilds were derived from studies conducted in the GOM in the 1980 s, recent diet analyses of the same species examined by Hopkins et al. (1996) suggests that the feeding patterns of many species is conserved (McClain-Counts et al., 2017; Olivar et al., 2019; Woodstock et al., 2020).

2.5. Median depth of occurrence determination for micronekton

To investigate the effect of depth on $\delta^{13}C$ and $\delta^{15}N$ values of micronekton, approximate median depth of occurrence for each species was estimated from the primary literature or from data collected during DEEPEND sampling. To attain the highest resolution data possible, we used data from studies employing opening and closing trawls only (MOCNESS, Tucker Trawl). Data from open net trawls, where the relative capture location of an individual within a large swath of the water column (greater than 400 m) could not be determined, were not considered. If multiple discrete-depth vertical distribution data sets were available, priority was given to studies reporting vertical

Table 2
Description of feeding guilds used to classify micronekton feeding habits. Feeding guild descriptions are adapted from Hopkins et al. (1994, 1996).

Functional Group	Feeding Guild	Feeding Guild Description
Detritivore	Detritivore	Marine snow and other particulate organic matter including fecal pellets and discarded larvacean housings
Zooplanktivore	Zoop. 1	Predominantly small crustaceans, with copepods the highest contributing category
Zooplanktivore	Zoop. 2	Mixed crustacean diet with large contributions by both copepods and small euphausiids
Zooplanktivore	Zoop. 3	Mixed crustacean diet primarily comprised of euphausiids and decapod crustaceans
Zooplanktivore	Zoop. 4	Mixed crustacean diet with ostracods representing more than 40 % of prey biomass
Zooplanktivore	Zoop. 5	Mixed crustacean diet with amphipods representing more than 33 % of prey biomass
Zooplanktivore	Zoop. 6	Non-crustacean invertebrates predominant; gastropods and salps comprise more than 85 % of prey items
Zooplanktivore	Zoop. 7	Diet almost exclusively gastropods
Gelativore	Gelativore	Gelatinous prey items comprise more than 66 % of prey by biomass
Micronektivore	Micronektivore	Diet dominated by large decapod crustaceans, with fish and other miscellaneous prey supplementing
Micronektivore	Piscivore	Diet dominated by fishes which represent more than 80 % of prey items by number

distribution at the finest scale. Additionally, depth distribution data from studies conducted in the GOM were given preference over data from the Atlantic or Pacific oceans. The references used to identify the median depth of occurrence for each species are outlined in Supplemental Table S1.

2.6. Statistical analysis

Trophic structure of the micronekton assemblage was explored using hierarchical cluster analysis on per-species mean $\delta^{13}C$ and $\delta^{15}N$ values using Ward's minimum variance clustering (Ward 1963; Murtagh and Legendre, 2014). Statistically significant clusters were identified using similarity profile routines (SIMPROF) at a significance level of 0.05. Following cluster analysis, one-way analysis of variance (ANOVA) was used to examine patterns of isotopic differences among identified clusters. Assumptions of ANOVA were checked using Shapiro-Wilk test (normality) and Levene's test (homogeneity of variance). Following ANOVA, *a posteriori* differences among means were analyzed using Tukey's Honestly Significant Difference test (Tukey HSD). Standard ellipse areas (SEA), used as a data visualization tool, were created using the R package SIBER (Jackson et al., 2011). The estimated SEAs encompass 40 % of the isotope data for each trophic grouping and represent the core isotopic niche area (Jackson et al., 2011).

Multiple linear regressions were used to examine variation in the $\delta^{13}C$ and $\delta^{15}N$ values of migratory and non-migratory micronekton. Specifically, we examined the relationship between $\delta^{13}C$ and $\delta^{15}N$ and body length, median nighttime depth of occurrence, median daytime depth of occurrence, capture location (latitude and longitude), and water column depth, with sampling season (spring, summer), and water type (GCW, LCW) included as categorical variables. Multicollinearity between independent variables was assessed using Variance Inflation Factors (VIF). In cases where VIF was greater than 3.0, the relationship between collinear variables was evaluated using linear regression (Queen et al., 2002). If R^2 was greater than 0.6, the variables were considered correlated, and the inclusion of both variables had the potential to bias the model (Queen et al., 2002) For all models examined, the R^2 of correlated variables (VIF greater than 3.0) was < 0.6 suggesting both variables could be included in candidate models without affecting interpretation. A backwards model selection procedure was used to identify and remove non-significant independent variables, with candidate models assessed using the Akaike information criterion (AIC; Akaike, 1974). Interactions between retained independent variables frequently resulted in VIF scores greater than 3.0 due to structural multicollinearity. In these cases, continuous variables were centered by calculating the mean for each variable and then subtracting the mean from all observed values of that variable (Queen et al., 2002). Stepwise selection continued until the removal of a remaining predictor variable resulted in an increase in AIC. Non-significant terms (p greater than 0.05) retained in the final model were removed if model AIC was comparable (<2) after removal (Burnham and Anderson, 2002). Once a final model was selected, variable importance was assessed using the absolute value of the *t*-statistic (Kuhn, 2008). Normality for all multiple regression models were assessed visually using qqplots. All statistical analyses were performed in the R statistical environment version 4.0.2 (R Core Development Team 2020) using the R packages vegan, MASS, multcomp, stats, and ggplot2.

3. Results

In total, SIA was conducted on 472 individuals from 58 species of micronekton. Species mean $\delta^{13}C$ values encompassed a narrow range from −21.6 ‰ to −18.1 ‰, while species mean $\delta^{15}N$ values ranged between 5.0 ‰ and 11.5 ‰. Using the criteria outlined by Hopkins et al. (1996), eleven distinct feeding guilds spanning several putative food web levels, from detritivores to piscivores, were identified in the micronekton assemblage examined (Table 2).

To assess the degree to which trophic structure estimations derived from SIA data agree with estimations from SCA, individual micronekton $\delta^{13}C$ and $\delta^{15}N$ values were plotted according to feeding guild (Fig. 2). Generally, there was broad isotopic overlap among feeding guilds, with zooplankton guilds overlapping with each other and, in the case of guilds Zoop. 1 and Zoop. 2, overlapping with micronektivore and piscivore guilds (Fig. 2). Notably, the isotopic overlap between lower and higher order feeding guilds was caused by a broad range of $\delta^{15}N$ values for Zoop. 1 and Zoop. 2, which were greater than expected given their narrow dietary breadth. For instance, species with diets dominated by copepods (Zoop. 1) and copepods/euphausiids (Zoop. 2) were characterized by $\delta^{15}N$ values spanning 7.11 ‰ and 5.24 ‰, respectively, with individuals of each group characterized by values exceeding those of micronektivores and piscivores (Fig. 2). The broad range of $\delta^{15}N$ values observed in some zooplanktivorous guilds contradicts known diet information and suggests additional sources of variation are influencing the isotopic values of some zooplanktivorous species.

In contrast to the 11 feeding guilds identified using SCA data, cluster analysis yielded four significant clusters or trophic groupings (Fig. 3). Interestingly, species were not strictly clustered by feeding guild, with zooplanktivores clustering with micronektivores and piscivores (Fig. 3; CLUST-3 and CLUST-4), suggesting elevated $\delta^{13}C$ and $\delta^{15}N$ values in some zooplanktivores could be driven by undescribed feeding at higher trophic positions or the use of food webs with elevated isotopic baselines. Species assigned to CLUST-1 were characterized by lower $\delta^{13}C$ (cluster mean: −21.24 ‰ ± 0.65 ‰) and $\delta^{15}N$ values (cluster mean: 5.38 ‰ ± 0.49 ‰), while species assigned to CLUST-4 displayed higher $\delta^{13}C$ (cluster mean: −18.58 ± 0.49 ‰) and $\delta^{15}N$ values (cluster mean: 10.32 ‰ ± 0.91 ‰). CLUST-2 and CLUST-3 were characterized by $\delta^{13}C$ and $\delta^{15}N$ values intermediate to groups one and four, with $\delta^{15}N$ values enriching with each subsequent cluster (Fig. 3). Statistically significant differences in the isotopic signatures among the four clusters were detected (MANOVA: $F_{3,54} = 19.21$; $p < 0.001$), with differences among clusters detected for $\delta^{13}C$ (ANOVA: $F_{3,54} = 16.81$; $p < 0.001$) and $\delta^{15}N$ values (ANOVA: $F_{3,54} = 124.14$; $p < 0.001$). Multiple comparisons suggested $\delta^{15}N$ values were significantly different among all clusters (Shaffer's MCP; $p < 0.001$, for each), while differences in cluster $\delta^{13}C$ values were driven by higher $\delta^{13}C$ values in CLUST-4 and lower $\delta^{13}C$

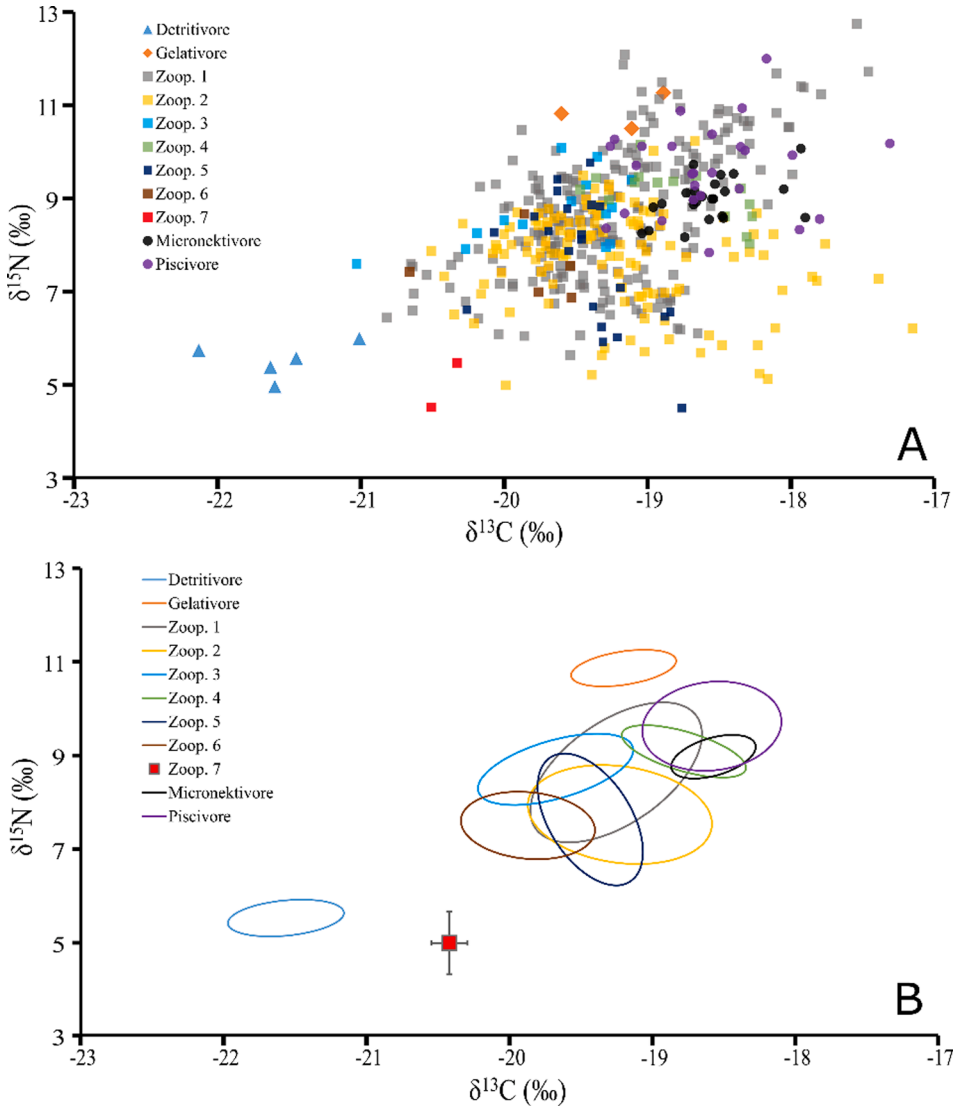

Fig. 2. (A) Individual $\delta^{13}C$ and $\delta^{15}N$ values of 58 species of micronekton grouped according to their assigned feeding guild. (B) Standard ellipse areas (SEAs) drawn to encompass ~ 40 % of $\delta^{13}C$ and $\delta^{15}N$ data for each feeding guild. Feeding guild Zoop. 7 is represented by mean $\delta^{13}C$ and $\delta^{15}N$ values (±s.d.) because estimation of SEA requires a minimum of three data points. For a description of feeding guilds, see Table 2.

values in CLUST-1 relative to all other clusters (Shaffer's MCP; $p < 0.001$, for each). Only CLUST-2 and CLUST-3 were found to have similar $\delta^{13}C$ values (Shaffer's MCP; $p = 0.23$).

3.1. *Multiple linear regression of $\delta^{13}C$ and $\delta^{15}N$ isotope values*

Results of multiple linear regression of $\delta^{13}C$ values for vertically migrating species yielded a best-fit model which included body length, water type, water column depth, and the interaction between body length and water type ($F_{4,261} = 22.50$; $p < 0.001$, $R^2 = 0.25$). For migrators, $\delta^{13}C$ values were slightly lower (a difference of 0.33 ‰) in GCW relative to LCW, increased with body length in both LCW and GCW and decreased with increasing water column depth (Fig. 4).

The best-fit model for $\delta^{13}C$ values of non-migrators included median nighttime depth, body length, water column depth, and the interactions between length and median nighttime depth, median nighttime depth and water type, and water column depth and water type ($F_{6,172} = 14.48$; $p < 0.001$, $R^2 = 0.31$). $\delta^{13}C$ values of non-migrators were positively correlated with median nighttime depth and body length, with the slope of the relationship between $\delta^{13}C$ and nighttime depth and between $\delta^{13}C$ and water column depth differing between water types (Fig. 5). Variable importance differed slightly between migratory and non-migratory species, with body length and water type identified as the most important variables for migratory species, while median nighttime depth and body length were the two most important variables in non-migratory species.

The best-fit model following multiple linear regression on $\delta^{15}N$ values of migratory species included body length, water type, median nighttime depth, median daytime depth, and interactions between body length and median nighttime depth, and median nighttime depth and water type ($F_{6,259} = 26.86$; $p < 0.001$, $R^2 = 0.37$). The $\delta^{15}N$ values of vertical migrators displayed a positive relationship with body length, median daytime depth, and median nighttime depth, with the slope of the relationship between $\delta^{15}N$ values and nighttime depth varying between LCW and GCW (Fig. 6). Additionally, the $\delta^{15}N$ values of vertical migrators were elevated in GCW relative to LCW. Vertical migrator $\delta^{15}N$ values were 0.45 ‰ higher in samples collected from GCW relative to samples from LCW. Although the averaged isotopic differences between LCW and GCW was < 1 ‰, there was considerable interspecific variation, with $\delta^{15}N$ values of some species differing by more than 2 ‰ between the two water masses.

The best-fit model for non-migratory species $\delta^{15}N$ values included

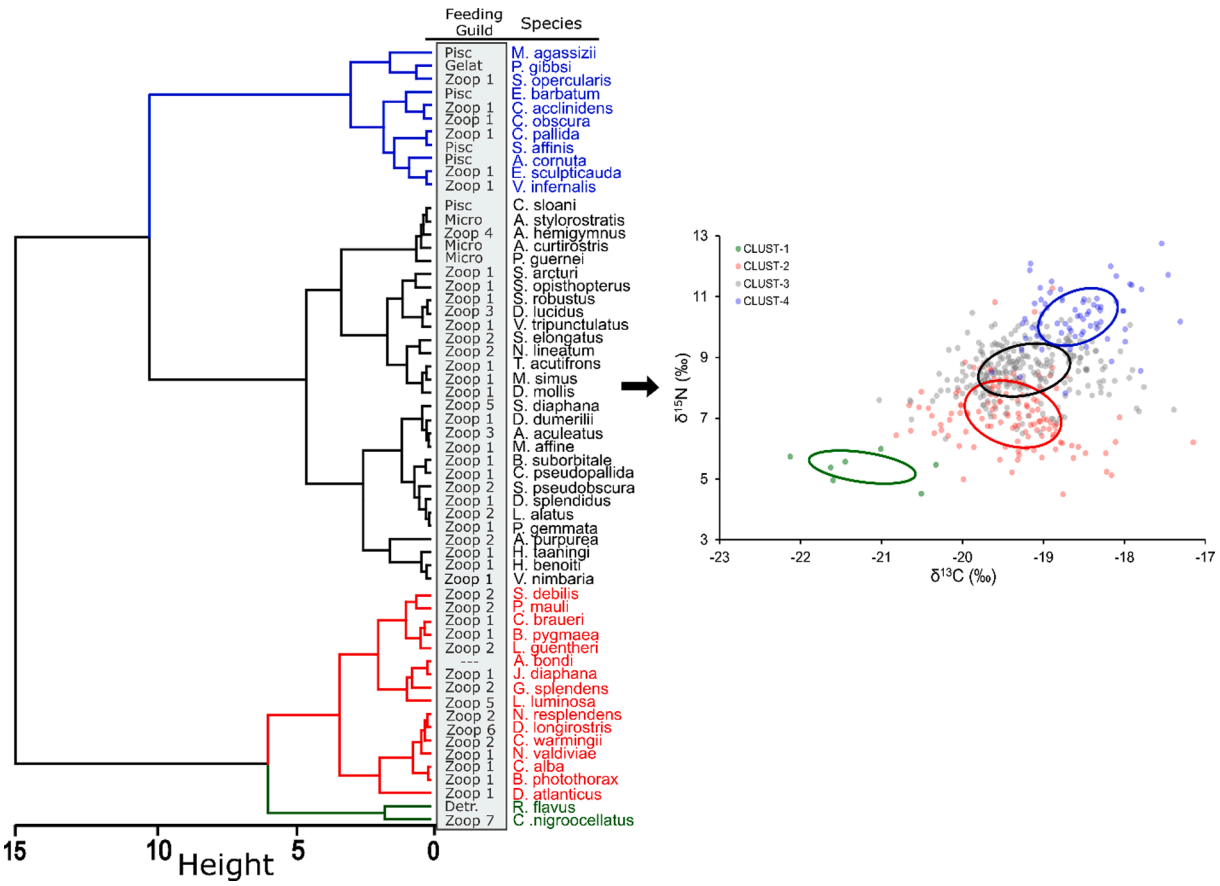

Fig. 3. Dendrogram of cluster analysis derived from per-species mean $\delta^{13}C$ and $\delta^{15}N$ values of micronekton (left panel). Colors represent statistically significant clusters identified through similarity profile routines (SIMPROF). The diet guild of each species is listed to illustrate discrepancies between stomach content and stable isotope data (zooplanktivores grouped with piscivores). Right Panel: Individual $\delta^{13}C$ and $\delta^{15}N$ values of 58 species of micronekton grouped according to cluster analysis and SIMPROF results. Ellipses represent the standard ellipse area (SEA) drawn to encompass ~ 40 % of the isotope data for each cluster.

median nighttime depth, body length, and the interaction between median nighttime depth and water column depth ($F_{3,175} = 39.52$; $p < 0.001$, $R^2 = 0.40$), with the $\delta^{15}N$ values of non-migrators positively correlated with median nighttime depth and body length (Fig. 7). Variable importance differed slightly between migratory and non-migratory species, with body length and water type the most important variables explaining $\delta^{15}N$ variation in migratory species, while median nighttime depth and body length were the two most important variables explaining variation in $\delta^{15}N$ values of non-migratory species. Detailed model outputs from each of the four final multiple linear regression models can be found in Supplemental Table S2.

3.2. Trophic position estimates

Mean TP:SIA estimates for the entire assemblage spanned two trophic levels between TP 2.6 (vertically migrating pteropod specialist *Centrobranchus nigroocellatus*) and TP 4.9 (non-migratory zooplanktivore *Eucopia sculpticauda*), with zooplanktivorous species (mean TP: 3.7) estimated to occupy a half trophic level below micronektivorous and piscivorous species (mean TP: 4.2). TP estimates were, on average, 0.3 and 0.4 TPs higher in non-migratory species relative to migratory species for zooplanktivores and micronektivores/piscivores, respectively (Fig. 8A). For both migratory and non-migratory species, TP:SIA estimates were generally higher than TP:SCA, although the magnitude of difference between the two methods varied between zooplanktivores and micronektivores/piscivores and between migration types (Fig. 8B). Specifically, the average difference between TP:SIA and TP:SCA estimates was 0.1 TLs and 0.5 TLs for migratory and non-migratory zooplanktivores, respectively, while the average difference in the two methods ranged between 0.1 and 0.4 TL for migratory and non-migratory piscivores/micronektivores, respectively (Fig. 8B). Because the precision between TP:SIA and TP:SCA varied by functional group and migration type, alignment between the two TP estimation methods varied among the major families of fishes examined, with precision increasing in families primarily comprising vertically migrating species. For instance, estimates between TP:SIA and TP:SCA differed on average by < 0.1 TLs for migratory myctophids and stomiids, while estimates between the two methods differed by an average of 0.6 TLs for non-migratory members of the families Sternoptychidae and Gonostomatidae.

4. Discussion

4.1. Trophic structure of the micronekton assemblage

Cluster analysis using stable isotope data of 58 micronekton species resulted in the identification of four trophic groups, which contrasted with the 11 feeding guilds identified using historical stomach content data (Hopkins et al., 1994; Hopkins et al., 1994). The lower number of trophic groupings identified using SIA was caused by the grouping of zooplanktivorous species known to feed on a range of taxa including copepods, euphausiids, ostracods, and amphipods (Hopkins et al., 1994; Hopkins et al. (1996)). The dissonance between the number of trophic groupings identified through SIA and SCA is driven by the contrasting taxonomic and temporal resolution of the two methods. SCA data can be influenced by seasonal prey availability, ontogenetic diet shifts, and random feeding events, resulting in high variation among individuals and species (Hopkins et al., 1996; Brush et al., 2012; Bernal et al., 2015).

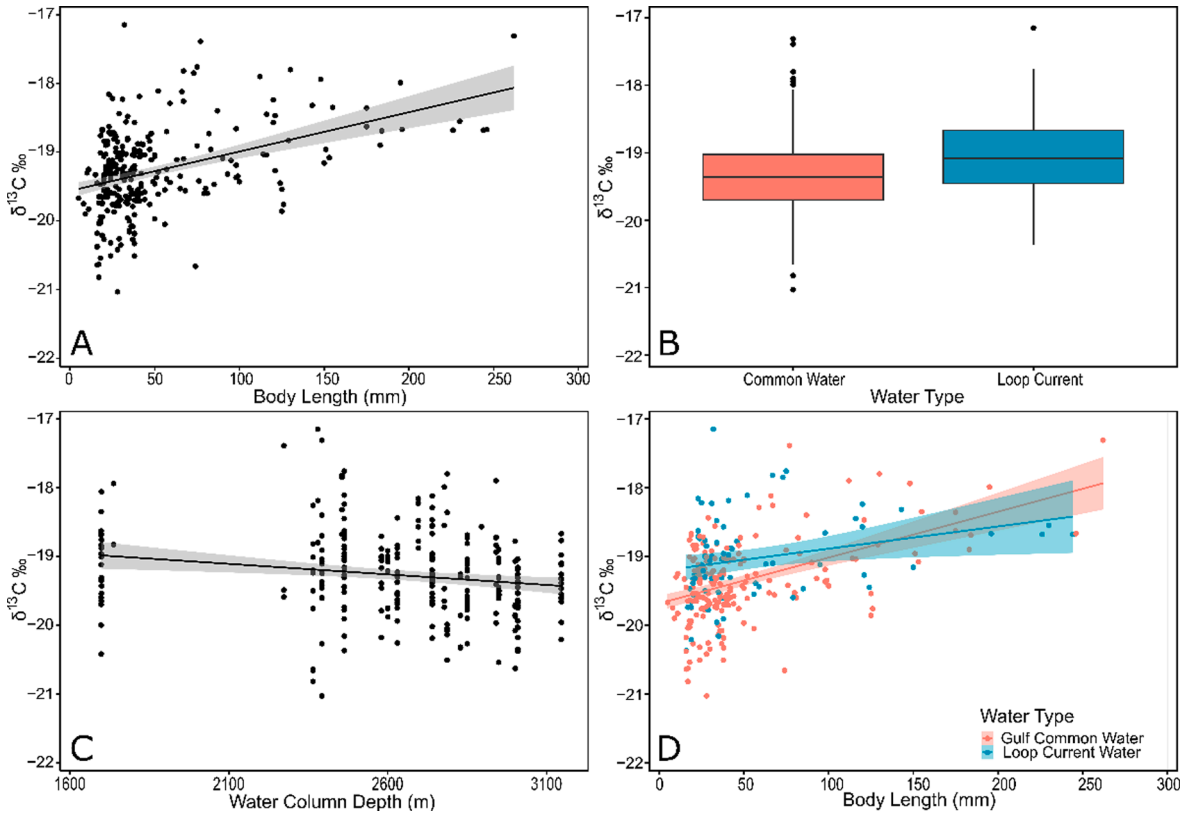

Fig. 4. Multiple linear regression results for $\delta^{13}C$ values of vertically migrating species relative to (A) body length, (B) water type, (C) water column depth, and (D) the interaction between body length and water type. Trend lines represent best fit lines for linear models, and gray bands represent 95% confidence intervals. Variables are ordered according to their relative importance in the final model.

Stable isotope ratios represent an "average" of an organism's feeding events resulting in lower variation among individuals and species. Additionally, isotopic variation is likely reduced in deep-pelagic systems where a single carbon source, phytoplankton, largely supports production of higher-order consumers (Choy et al., 2015; Drazen and Sutton, 2017; Gloeckler et al., 2018). Thus, in this and other studies of the deep pelagial, SCA may suggest that micronekton feed diversely and identify numerous trophic groupings, but the variable diets of micronekton may not translate to high isotopic variation, as all prey items share an isotopically similar carbon source.

The range of $\delta^{13}C$ values observed, which spanned a relatively narrow 3.4 ‰ between endmembers, aligns with previous examinations in the GOM (McClain-Counts et al., 2017) and tropical Atlantic Ocean (Czudaj et al., 2020), and suggests that the micronekton assemblage we sampled is largely supported by pelagic phytoplankton production. In contrast, we observed significant variation in $\delta^{15}N$ values (6.5 ‰ between endmember species) within the assemblage seemingly driven by interspecific differences in diet, vertical migratory behavior, and depth of occurrence. The effect of diet on the trophic structure of the GOM micronekton assemblage was evident in the results of the cluster analysis. Migratory and non-migratory piscivores, characterized by high $\delta^{15}N$ values, clustered together at the top of the assemblage, while most zooplanktivores, regardless of vertical migration, were grouped between the piscivores and the detritivore *Rhynchoconger flavus*. However, some non-migratory zooplanktivores, including several members of the genus *Cyclothone*, the vampire squid *Vampyroteuthis infernalis*, the bathypelagic euphausiid *E. sculpticauda*, and the bigscale *Scopeloberyx opercularis*, possessed $\delta^{15}N$ values that were equal to or exceeded those of known piscivores. The elevated $\delta^{15}N$ values in these deep-dwelling non-migratory species (average median nighttime depth: 1300 m) counter available diet data and suggest these species feed at depth in food webs supported by degraded particulate organic matter (POM) with an elevated ^{15}N signature (Gloeckler et al., 2018). Stable isotope examinations of POM, often used as a proxy for phytoplankton, have shown that as POM sinks, bacterial degradation results in the removal of isotopically light nitrogen (^{14}N), leaving the residual material isotopically enriched relative to POM at shallower depths (Mintenbeck et al., 2007; Hannides et al., 2013). This bacterial degradation results in POM collected from the lower *meso-* and bathypelagic zone being characterized by $\delta^{15}N$ values that can be 3–10 ‰ higher than newly formed POM collected near the surface (Altabet, 1988). Subsequent studies have shown that the elevated $\delta^{15}N$ values of POM in the lower *meso-* and bathypelagic zones can be reflected in micronekton occupying similar depths, resulting in zooplanktivores with $\delta^{15}N$ signatures similar to piscivorous species supported by POM with lower $\delta^{15}N$ values in the epipelagic zone (Hannides et al., 2013, Gloeckler et al., 2018; Richards et al., 2020).

4.2. Depth of occurrence

The effect of depth of occurrence, which was detectable in the clustering of deeper-dwelling zooplanktivores with piscivores, was also evident in the results of multiple linear regression analysis. Specifically, the $\delta^{13}C$ and $\delta^{15}N$ values of non-migrators and the $\delta^{15}N$ values of vertical migrators were positively correlated with increasing median nighttime depth of occurrence. Within non-migratory species, it's notable that the relationship between $\delta^{15}N$ and depth was not driven by larger, higher trophic level predators occupying deeper depths, as small-bodied zooplanktivores occupied the deepest depths of the assemblage. Despite the clear relationship between $\delta^{15}N$ values and nighttime depth of occurrence in non-migrators, we did observe a wide range of $\delta^{15}N$ values among species inhabiting similar depths (Fig. 7A). For instance, zooplanktivores of similar sizes occupying nighttime depths between 900 and 1050 m possessed mean $\delta^{15}N$ values that ranged from 8.1 ‰

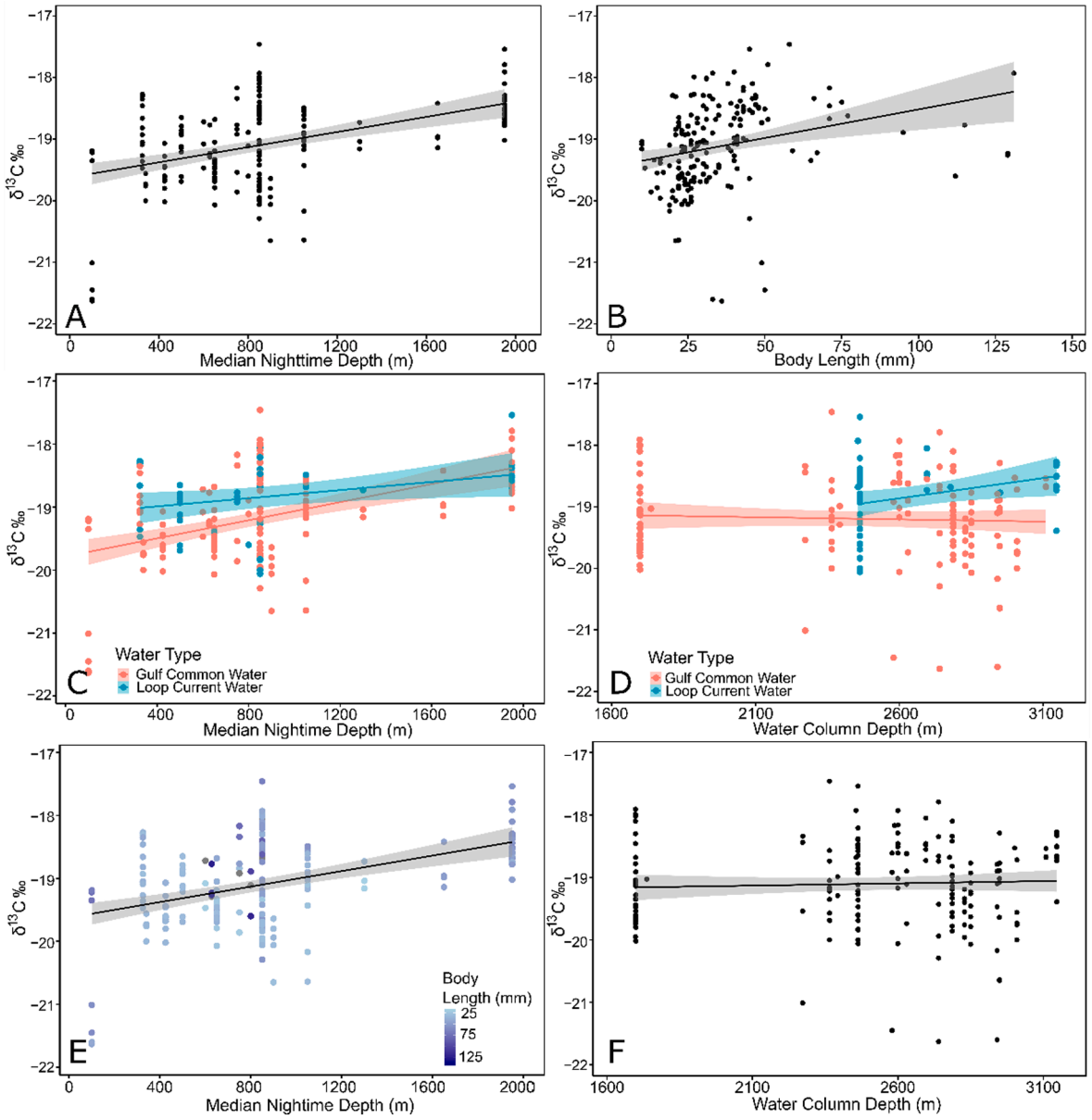

Fig. 5. Multiple linear regression results for $\delta^{13}C$ values of non-migratory species relative to (A) median nighttime depth of occurrence, (B) body length, (C) the interaction between median nighttime depth of occurrence and water type, (D) the interaction between water column depth and water type, (E) the interaction between median nighttime depth and body length, and (F) water column depth. Trend lines represent best fit lines for linear models and gray bands represent 95% confidence intervals. Variables are ordered according to their relative importance in the final model.

(*Sternoptyx pseudobscura*) to 11.1 ‰ (*S. opercularis*). Additionally, non-migratory zooplanktivores displayed $\delta^{15}N$ values similar to non-migratory piscivores at similar depths. This variation among non-migratory species suggests that the use of ^{15}N enriched baselines within the mesopelagic zone is not solely determined by depth and can vary by species and functional group (Gloeckler et al., 2018). Currently, our data and evidence from other studies of deep-pelagic trophic structure suggests that the use of isotopically enriched baselines is most common in lower-trophic level non-migratory species inhabiting depths greater than ~ 1000 m in the bathypelagic zone (Gloeckler et al., 2018; Richards et al., 2020; Bode et al., 2021).

Median nighttime depth was also significantly correlated with $\delta^{15}N$ values in migratory species (Fig. 6D), but the relationship was not as pronounced relative to non-migratory taxa. Contrary to non-migratory species, vertically migrating species mainly feed at night in the epipelagic zone where the isotopic signatures of POM particles are relatively uniform, which helps reduce the likelihood of species utilizing food webs with differing isotopic baselines (Hopkins et al., 1996; Drazen and Sutton, 2017; Gloeckler et al., 2018). Additionally, the relationship observed between $\delta^{15}N$ values and depth of occurrence in vertical migrators is driven in part by higher-trophic level species occupying the deepest depths of the assemblage (Table 1). Many of these piscivorous species (e.g *Chauliodus sloani, Echiostoma barbatum, Stomias affinis*) are asynchronous vertical migrators, with only a portion of the population migrating upward at night to feed, while the remaining individuals remain in the *meso-* or bathypelagic (Sutton and Hopkins, 1996a; Sutton and Hopkins, 1996b). This asynchronous migration pattern results in a deeper median nighttime depth of occurrence despite evidence that suggests these species largely feed when they migrate vertically into the epipelagic zone (Sutton and Hopkins, 1996b; Richards et al., 2019). The conclusion that depth of occurrence more strongly influences the trophic structure of non-migratory species is consistent with previous examinations of micronekton trophic structure in the Pacific Ocean (Gloeckler et al., 2018; Romero-Romero et al., 2019), Mediterranean (Valls et al.,

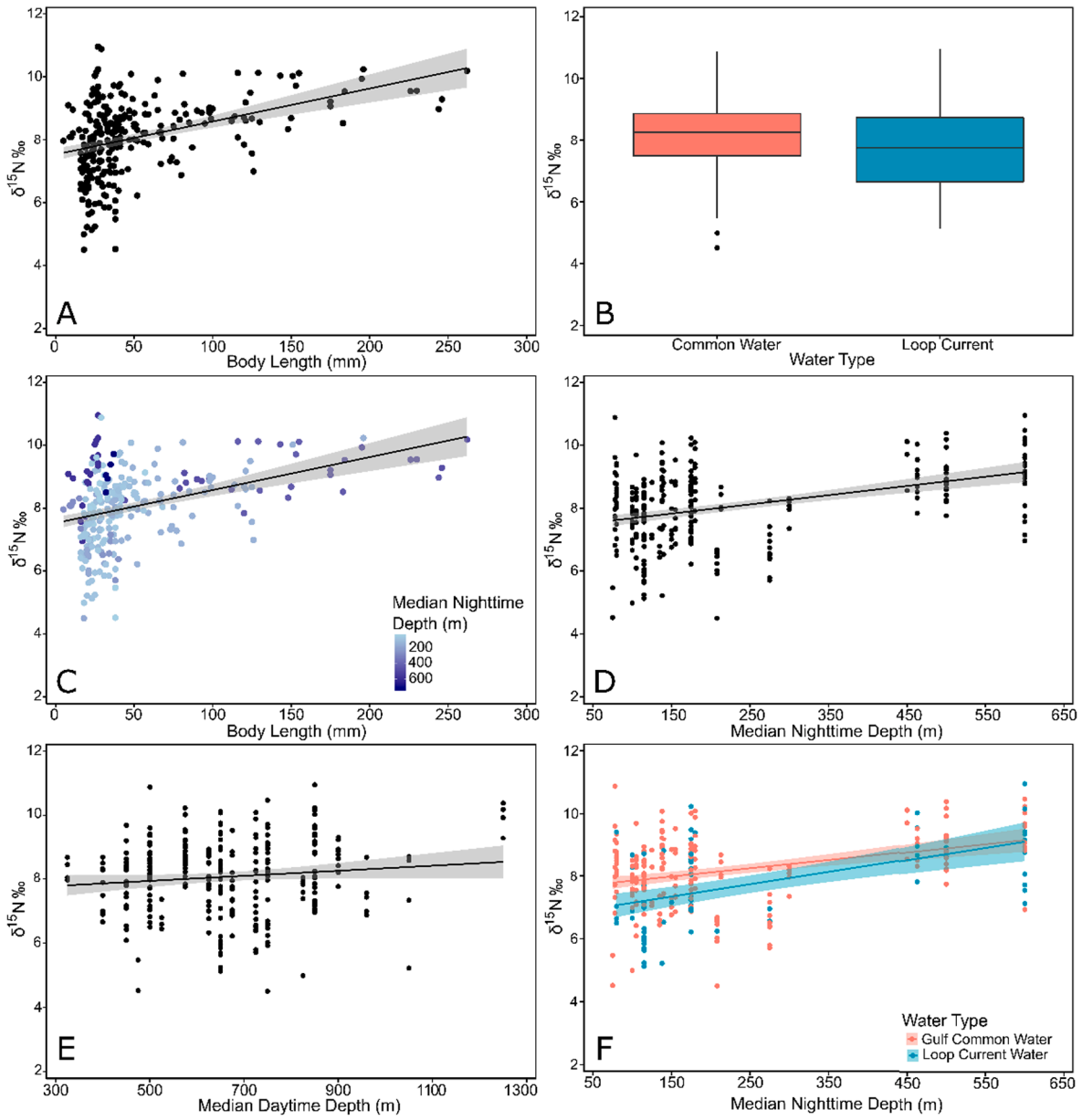

Fig. 6. Multiple linear regression results for $\delta^{15}N$ values of vertically migrating species relative to (A) body length, (B) water type, (C) interaction between body length and median nighttime depth of occurrence, (D) median nighttime depth of occurrence, (E) median daytime depth of occurrence, and (F) the interaction between median nighttime depth of occurrence and water type. Trend lines represent best fit lines for linear models, and gray bands represent 95 % confidence intervals. Variables are ordered according to their relative importance in the final model.

2014), Atlantic Ocean (Parzanini et al., 2017; Czudaj et al., 2020; Bode et al., 2021), and GOM (Richards et al., 2020) and suggests depth is likely an important driver of trophic structure in low-latitude oligotrophic ecosystems worldwide.

4.3. Body length

Body length was retained in all final models and was identified as the most important factor explaining isotopic variation in migrating species and the second most important factor in non-migrators. Analysis of stomach contents suggests that feeding habits of both migrating and non-migrating GOM micronekton are highly size structured, with the type and size of prey changing and increasing in species with larger body and gape sizes (Hopkins and Gartner, 1992; Hopkins et al., 1994; Hopkins et al., 1996; Sutton and Hopkins 1996a). Body size is one of the most important factors structuring marine food webs and is clearly an important factor influencing the trophic structure of migratory and non-migratory deep-pelagic micronekton in the GOM as well (Jennings et al., 2001; Romero-Romero et al., 2016; Romero-Romero et al., 2019). As mentioned above, the apparent difference in the relative importance of body length in explaining isotopic variation of migrators and non-migrators is driven by differences in feeding location within the water column, with non-migratory species more likely to use food webs with enriched nitrogen baselines at depth while migratory species feed within food webs with similar isotopic baselines (Hopkins et al., 1996; Sutton and Hopkins, 1996a).

4.4. Water type

The final regression models for migratory species included water type, although the factor was of lesser importance in explaining isotopic variation relative to body length. The observed pattern of higher $\delta^{13}C$

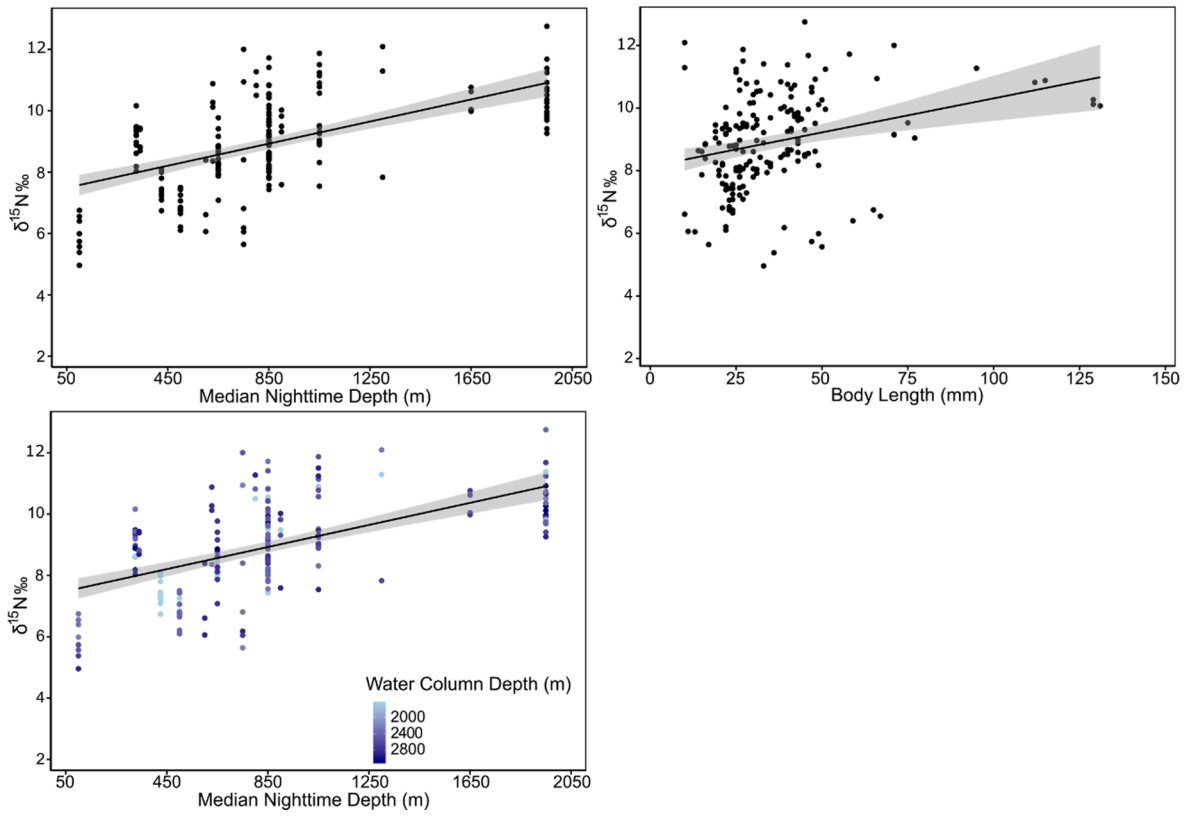

Fig. 7. Multiple linear regression results for $\delta^{15}N$ values of non-migratory species relative to median nighttime depth of occurrence (A), body length (B), and the interaction between median nighttime depth and water depth (C). Trend lines represent best fit lines for linear models, and gray bands represent 95 % confidence intervals. Variables are ordered according to their relative importance in the final model.

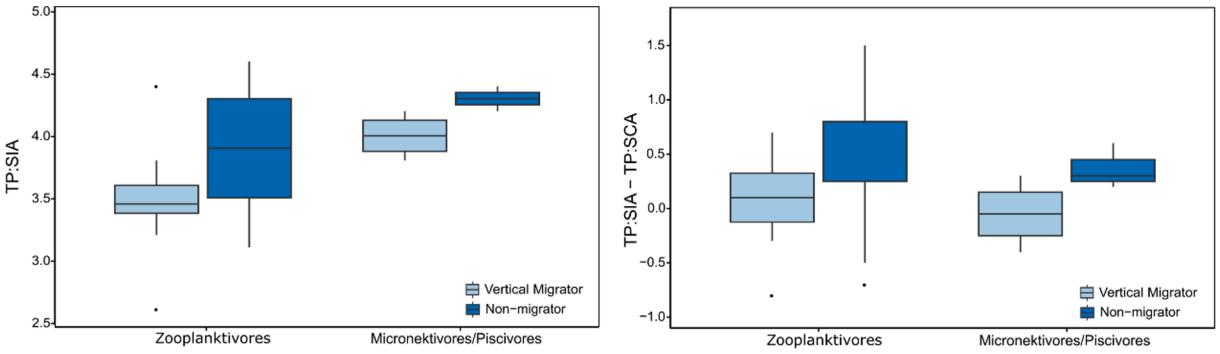

Fig. 8. (A) Boxplots depicting differences in stable isotope trophic position estimates (TP: SIA) of vertically migrating (light blue) and non-migratory (dark blue) zooplanktivores and micronektivores/piscivores. (B) Boxplots depicting differences in TP:SIA and trophic position estimates made using stomach content analysis (TP:SCA) for vertically migrating and non-migratory zooplanktivores and micronektivores/piscivores. Boxplots represent 25th%, 50th% and 75th% percentile, while whisker lengths represent 1.5*interquartile range.

and lower $\delta^{15}N$ values in LCW relative to GCW has been demonstrated previously in epipelagic POM, zooplankton and micronekton in the GOM (Wells et al., 2017; Richards et al., 2020). Differences in the isotopic composition of consumers collected from the two water masses is driven by differences in sources of nitrogen fueling the base of the food web (Biggs, 1992). The waters of the anticyclonic Loop Current are characterized by deep nitracline depths, which result in primary production in the epipelagic primarily relying on isotopically light nitrogen derived from nitrogen fixing cyanobacteria *Trichodesmium* spp. which is characterized by enriched $\delta^{13}C$ values relative to POM in GCW (Montoya et al., 2002; Dorado et al., 2012; Wells et al., 2017). In contrast, primary production in neritic waters (i.e., GCW) is largely supported by isotopically enriched deep-water nitrate with higher $\delta^{15}N$ and lower $\delta^{13}C$ values which are then reflected in the isotopic signatures of consumers (Biggs, 1992; Wells et al., 2017; Olivar et al., 2019).

Notably, the main effect of water type was not retained in either model for non-migratory species suggesting the likelihood of a consumer carrying a water mass-specific isotopic signature may decrease with increasing depth. The potential effect of depth on isotopic differences between water masses can also be seen in the interactions between water type and median nighttime depth retained in the final models for migratory $\delta^{15}N$ and non-migratory $\delta^{13}C$. In both instances, the differences in slope between the regression lines for LCW and GCW were greatest at shallower depths, with isotopic differences between the two water masses diminishing with depth. The Loop Current dominates circulation in near-surface waters of the GOM but use of unique salinity-

temperature-depth profiles inherent to LCW and GCW demonstrated that substantial mixing between the two water masses begins in the upper-mesopelagic (Cardona and Bracco, 2016; Johnston et al., 2019). Thus, it is possible that species foraging within the upper or lower-mesopelagic are less likely to incorporate isotopic signatures specific to a water mass. While the isotopic differences between water masses is interesting, low sample sizes in LCW hampered our ability to run detailed analyses and results should be interpreted with caution. However, previous evidence detecting differences between the two water masses (Biggs, 1992; Wells et al., 2017; Johnston et al., 2019) combined with our detection of isotopic differences between water masses despite the trophic and life history variation in the assemblage warrants more detailed examination. Further, these results support the use of more precise methods for estimating trophic positions, such as amino acid compound specific isotope analysis, which allow for isotopic baseline integration in a single sample (e.g. Choy et al., 2012; Bode et al., 2021).

4.5. Trophic position estimates

The trophic position estimates for deep-pelagic micronekton, which spanned two trophic levels between 2.6 and 4.8, were similar to estimations in the GOM, Atlantic, and Pacific oceans (Choy et al., 2013; McClain-Counts et al., 2017). Although average TP estimates were higher for micronektivores and piscivores (mean TL: 4.2) relative to zooplanktivores (mean TL: 3.7), there was considerable overlap in TP estimations between the two groups suggesting tight trophic linkages within the GOM micronekton assemblage. In general, relative to published TP:SCA values, TP:SIA estimations were overestimated to a greater extent in non-migrators, with greater disagreement between the two methods for zooplanktivores. The higher trophic position estimates of non-migratory taxa derived from SIA likely stem from increased reliance on food webs supported by enriched isotopic baselines at depth, suggesting that the pyrosome, *P. atlanticum*, does not adequately characterize the nitrogen baseline for some deeper dwelling, non-migratory species. Despite overestimations in TP:SIA in non-migrators, TP:SIA estimations agreed well with TP:SCA in migratory species, suggesting *P. atlanticum* is suitable for delineating the nitrogen baseline for migratory species in the GOM. The agreement between the two methods in migratory taxa is useful as it suggests that TP:SIA, which requires fewer samples and is a more accessible method (less reliance on taxonomic expertise and intact stomach contents), adequately describes trophic positions for a variety of ecologically important groups including myctophids and stomiids. Although it is tempting to use an alternative baseline such as POM collected from the *meso-* or bathypelagic to estimate TPs of non-migratory species, the high level of observed variation in $\delta^{15}N$ values in non-migratory species suggests that relative use of isotopically enriched baselines varies by species so a "one size fits all" approach is unlikely to adequately describe trophic positions.

4.6. Conclusions

In summary, through the combined use of bulk SIA data and historical SCA data, we shed light on the factors shaping the trophic structure of deep-pelagic micronekton assemblages in the GOM. Estimations of trophic structure made with SIA were simpler and identified fewer trophic groupings relative to estimations made using SCA and suggested isotopic variation among most consumers occurs along the $\delta^{15}N$ axis. The contrasting depictions of trophic structure provided by SIA and SCA underscore the utility of combining the two methods. Within the micronekton assemblage, we found that body size, nighttime depth of occurrence, and proximity to the dominant mesoscale oceanographic feature, the Loop Current, were important drivers of trophic structure. Notably, the relative importance of these factors varied between vertically migrating and non-migratory species. Body size and proximity to the Loop Current were identified as the most important factors to migrators while nighttime depth of occurrence and body size were the most important factors explaining variation among non-migrators. The positive relationship between $\delta^{15}N$ and nighttime depth of occurrence observed in non-migrators suggests that at deeper depths some zooplanktivorous species feed within food webs supported by isotopically enriched POM. The use of elevated isotopic baselines in deeper dwelling species is important as it can lead to the overestimation of trophic position for some consumers.

Funding

This work was supported by a grant from The Gulf of Mexico Research Initiative. All isotope and metadata are available through Dryad using the https://doi.org/10.7291/D1T10D.

Declaration of Competing Interest

The authors declare that they have no known competing financial interests or personal relationships that could have appeared to influence the work reported in this paper.

Data availability

Data are publicly available through Dryad:https://datadryad.org/stash/share/YWDq8QGS4qmdf02iq6QQ_JgWZ0uNN1Sr_lvVWpWxV8Y

Acknowledgments

We would like to thank the crew of the r/v Point Sur for their help operating the MOCNESS. We are grateful to April Cook for her organization of the DEEPEND micronekton database and to Matthew Johnston for his help with GIS. We would also like to thank the members of the Wells Shark Biology and Fisheries Science Lab for their support and feedback during the writing of this manuscript. This paper is a result of research funded by the Gulf of Mexico Research Initiative and the National Oceanic and Atmospheric Administration's RESTORE Science Program under award NA19NOS4510193 to Nova Southeastern University.

Appendix A. Supplementary material

Supplementary data to this article can be found online at https://doi.org/10.1016/j.pocean.2023.102998.

References

Akaike, H., 1974. A new look at the statistical model identification. IEEE Trans. Autom. Control 19 (6), 716–723.
Altabet, M.A., 1988. Variations in nitrogen isotopic composition between sinking and suspended particles: implications for nitrogen cycling and particle transformation in the open ocean. Deep Sea Res. Part A 35 (4), 535–554.
Bangma, J.L., Haedrich, R.L., 2008. Distinctiveness of the mesopelagic fish fauna in the Gulf of Mexico. Deep Sea Res. Part II 55 (24–26), 2594–2596.
Behrenfeld, M.J., Gaube, P., Della Penna, A., O'Malley, R.T., Burt, W.J., Hu, Y., Doney, S. C., 2019. Global satellite-observed daily vertical migrations of ocean animals. Nature 576 (7786), 257–261.
Bernal, A., Olivar, M.P., Maynou, F., de Puelles, M.L.F., 2015. Diet and feeding strategies of mesopelagic fishes in the western Mediterranean. Prog. Oceanogr. 135, 1–17.
Biggs, D.C., 1992. Nutrients, plankton, and productivity in a warm-core ring in the western Gulf of Mexico. J. Geophys. Res. Oceans 97 (C2), 2143–2154.
Bode, A., Olivar, M.P., Hernández-León, S., 2021. Trophic indices for micronektonic fishes reveal their dependence on the microbial system in the North Atlantic. Sci. Rep. 11 (1), 1–10.
Brierley, A.S., 2014. Diel vertical migration. *Curr. Biol.* 24 (22), R1074–R1076.
Brush, J.M., Fisk, A.T., Hussey, N.E., Johnson, T.B., 2012. Spatial and seasonal variability in the diet of round goby (Neogobius melanostomus): stable isotopes indicate that stomach contents overestimate the importance of dreissenids. Can. J. Fish. Aquat. Sci. 69 (3), 573–586.
Bunn, S.E., Loneragan, N.R., Kempster, M.A., 1995. Effects of acid washing on stable isotope ratios of C and N in penaeid shrimp and seagrass: Implications for food-web studies using multiple stable isotopes. Limnol. Oceanogr. 40 (3), 622–625.

Burghart, S.E., Hopkins, T.L., Torres, J.J., 2010. Partitioning of food resources in bathypelagic micronekton in the eastern Gulf of Mexico. Mar. Ecol. Prog. Ser. 399, 131–140.
Burnham, K.P., Anderson, D.R., 2002. Model selection and multimodel inference: a practical information-theoretic approach. Springer, New York, NY.
Cardona, Y., Bracco, A., 2016. Predictability of mesoscale circulation throughout the water column in the Gulf of Mexico. Deep Sea Res. Part II 129, 332–349.
Caut, S., Angulo, E., Courchamp, F., 2009. Variation in discrimination factors (Δ15N and Δ13C): the effect of diet isotopic values and applications for diet reconstruction. J. Appl. Ecol. 46 (2), 443–453.
Cherel, Y., Fontaine, C., Richard, P., Labatc, J.P., 2010. Isotopic niches and trophic levels of myctophid fishes and their predators in the Southern Ocean. Limnol. Oceanogr. 55 (1), 324–332.
Choy, C.A., Davison, P.C., Drazen, J.C., Flynn, A., Gier, E.J., Hoffman, J.C., McClain-Counts, J.P., et al., 2012. Global trophic position comparison of two dominant mesopelagic fish families (Myctophidae, Stomiidae) using amino acid nitrogen isotopic analyses. PLoS One 7 (11), e50133.
Choy, C.A., Portner, E., Iwane, M., Drazen, J.C., 2013. Diets of five important predatory mesopelagic fishes of the central North Pacific. Mar. Ecol. Prog. Ser. 492, 169–184.
Choy, C.A., Popp, B.N., Hannides, C.C.S., Drazen, J.C., 2015. Trophic structure and food resources of epipelagic and mesopelagic fishes in the North Pacific Subtropical Gyre ecosystem inferred from nitrogen isotopic compositions. Limnol. Oceanogr. 60 (4), 1156–1171.
Choy, C.A., Wabnitz, C.C., Weijerman, M., Woodworth-Jefcoats, P.A., Polovina, J.J., 2016. Finding the way to the top: how the composition of oceanic mid-trophic micronekton groups determines apex predator biomass in the central North Pacific. Mar. Ecol. Prog. Ser. 549, 9–25.
Cook, A. B., Bernard, A. M., Boswell, K. M., Bracken-Grissom, H., D'Elia, M., DeRada, S., ... & Sutton, T. T. (2020). A Multidisciplinary approach to investigate deep-pelagic ecosystem dynamics in the Gulf of Mexico following Deepwater Horizon. *Frontiers in Marine Science*, 1122.
Czudaj, S., Giesemann, A., Hoving, H.J., Koppelmann, R., Lüskow, F., Möllmann, C., Fock, H.O., 2020. Spatial variation in the trophic structure of micronekton assemblages from the eastern tropical North Atlantic in two regions of differing productivity and oxygen environments. Deep Sea Res. Part I 163, 103275.
Davis, R.W., Ortega-Ortiz, J.G., Ribic, C.A., Evans, W.E., Biggs, D.C., Ressler, P.H., et al., 2002. Cetacean habitat in the northern oceanic Gulf of Mexico. Deep Sea Res. Part I 49 (1), 121–142.
Davison, P.C., Checkley Jr, D.M., Koslow, J.A., Barlow, J., 2013. Carbon export mediated by mesopelagic fishes in the northeast Pacific Ocean. Prog. Oceanogr. 116, 14–30.
DeNiro, M.J., Epstein, S., 1978. Influence of diet on the distribution of carbon isotopes in animals. Geochim. Cosmochim. Acta 42 (5), 495–506.
Dittel, A.I., Epifanio, C.E., Cifuentes, L.A., Kirchman, D.L., 1997. Carbon and nitrogen sources for shrimp postlarvae fed natural diets from a tropical mangrove system. Estuar. Coast. Shelf Sci. 45 (5), 629–637.
Dorado, S., Rooker, J.R., Wissel, B., Quigg, A., 2012. Isotope baseline shifts in pelagic food webs of the Gulf of Mexico. Mar. Ecol. Prog. Ser. 464, 37–49.
Downs, E.E., Popp, B.N., Holl, C.M., 2014. Nitrogen isotope fractionation and amino acid turnover rates in the Pacific white shrimp Litopenaeus vannamei. Mar. Ecol. Prog. Ser. 516, 239–250.
Drazen, J.C., Sutton, T.T., 2017. Dining in the deep: the feeding ecology of deep-sea fishes. Ann. Rev. Mar. Sci. 9, 337–366.
Drazen, J.C., Smith, C.R., Gjerde, K.M., Haddock, S.H., Carter, G.S., Choy, C.A., Yamamoto, H., 2020. Opinion: midwater ecosystems must be considered when evaluating environmental risks of deep-sea mining. Proc. Natl. Acad. Sci. 117 (30), 17455–17460.
Eduardo, L. N., Lucena-Frédou, F., Mincarone, M. M., Soares, A., Le Loc'h, F., Frédou, T., ... & Bertrand, A. (2020). Trophic ecology, habitat, and migratory behaviour of the viperfish Chauliodus sloani reveal a key mesopelagic player. *Scientific reports*, *10*(1), 1-13.
Froese, R., & Pauly, D. (2010). FishBase.
Gloeckler, K., Choy, C.A., Hannides, C.C., Close, H.G., Goetze, E., Popp, B.N., Drazen, J. C., 2018. Stable isotope analysis of micronekton around Hawaii reveals suspended particles are an important nutritional source in the lower mesopelagic and upper bathypelagic zones. Limnol. Oceanogr. 63 (3), 1168–1180.
Hannides, C.C., Popp, B.N., Choy, C.A., Drazen, J.C., 2013. Midwater zooplankton and suspended particle dynamics in the North Pacific Subtropical Gyre: a stable isotope perspective. Limnol. Oceanogr. 58 (6), 1931–1946.
Hesslein, R.H., Hallard, K.A., Ramlal, P., 1993. Replacement of sulfur, carbon, and nitrogen in tissue of growing broad whitefish (Coregonus nasus) in response to a change in diet traced by δ34S, δ13C, and δ15N. Can. J. Fish. Aquat. Sci. 50 (10), 2071–2076.
Holl, C.M., Villareal, T.A., Payne, C.D., Clayton, T.D., Hart, C., Montoya, J.P., 2007. Trichodesmium in the western Gulf of Mexico: 15N2-fixation and natural abundance stable isotopic evidence. Limnol. Oceanogr. 52 (5), 2249–2259.
Hopkins, T.L., Flock, M.E., Gartner Jr, J.V., Torres, J.J., 1994. Structure and trophic ecology of a low latitude midwater decapod and mysid assemblage. Mar. Ecol. Prog. Ser. 143–156.
Hopkins, T.L., Gartner, J.V., 1992. Resource-partitioning and predation impact of a low-latitude myctophid community. Mar. Biol. 114 (2), 185–197.
Hopkins, T.L., Sutton, T.T., Lancraft, T.M., 1996. The trophic structure and predation impact of a low latitude midwater fish assemblage. Prog. Oceanogr. 38 (3), 205–239.
Hussey, N.E., MacNeil, M.A., McMeans, B.C., Olin, J.A., Dudley, S.F., Cliff, G., Fisk, A.T., 2014. Rescaling the trophic structure of marine food webs. Ecol. Lett. 17 (2), 239–250.
Hyslop, E.J., 1980. Stomach contents analysis—a review of methods and their application. J. Fish Biol. 17 (4), 411–429.
Irigoien, X., Klevjer, T.A., Røstad, A., Martinez, U., Boyra, G., Acuña, J.L., et al., 2014. Large mesopelagic fishes biomass and trophic efficiency in the open ocean. Nat. Commun. 5 (1), 1–10.
Jackson, A.L., Inger, R., Parnell, A.C., Bearhop, S., 2011. Comparing isotopic niche widths among and within communities: SIBER – Stable Isotope Bayesian Ellipses in R. J. Anim. Ecol. 80, 595–602.
Jennings, S., Pinnegar, J.K., Polunin, N.V., Boon, T.W., 2001. Weak cross-species relationships between body size and trophic level belie powerful size-based trophic structuring in fish communities. J. Anim. Ecol. 934–944.
Johnston, M.W., Milligan, R.J., Easson, C.G., DeRada, S., English, D.C., Penta, B., Sutton, T.T., 2019. An empirically validated method for characterizing pelagic habitats in the Gulf of Mexico using ocean model data. Limnol. Oceanogr. Methods 17 (6), 362–375.
Kuhn, M., 2008. Building predictive models in R using the caret package. J. Stat. Softw. 28 (1), 1–26.
MacAvoy, S.E., Macko, S.A., Garman, G.C., 2001. Isotopic turnover in aquatic predators: quantifying the exploitation of migratory prey. Can. J. Fish. Aquat. Sci. 58 (5), 923–932.
Mancinelli, G., Vizzini, S., Mazzola, A., Maci, S., Basset, A., 2013. Cross-validation of δ15N and FishBase estimates of fish trophic position in a Mediterranean lagoon: the importance of the isotopic baseline. Estuar. Coast. Shelf Sci. 135, 77–85.
McClain-Counts, J.P., Demopoulos, A.W., Ross, S.W., 2017. Trophic structure of mesopelagic fishes in the Gulf of Mexico revealed by gut content and stable isotope analyses. Mar. Ecol. 38 (4), e12449.
Mengerink, K.J., Van Dover, C.L., Ardron, J., Baker, M., Escobar-Briones, E., Gjerde, K., et al., 2014. A call for deep-ocean stewardship. Science 344 (6185), 696–698.
Milligan, R.J., Bernard, A.M., Boswell, K.M., Bracken-Grissom, H.D., D'Elia, M.A., DeRada, S., et al., 2018. The application of novel research technologies by the deep pelagic nekton dynamics of the Gulf of Mexico (DEEPEND) Consortium. Marine Technol. Soc. J. 52 (6), 81–86.
Minagawa, M., Wada, E., 1984. Stepwise enrichment of 15N along food chains: further evidence and the relation between δ^{15}N and animal age. Geochim. Cosmochim. Acta 48 (5), 1135–1140.
Mintenbeck, K., Jacob, U., Knust, R., Arntz, W.E., Brey, T., 2007. Depth-dependence in stable isotope ratio δ^{15}N of benthic POM consumers: the role of particle dynamics and organism trophic guild. Deep Sea Res. Part I 54 (6), 1015–1023.
Montoya, J.P., Carpenter, E.J., Capone, D.G., 2002. Nitrogen fixation and nitrogen isotope abundances in zooplankton of the oligotrophic North Atlantic. Limnol. Oceanogr. 47 (6), 1617–1628.
Moteki, M., Arai, M., Tsuchiya, K., Okamoto, H., 2001. Composition of piscine prey in the diet of large pelagic fish in the eastern tropical Pacific Ocean. Fish. Sci. 67 (6), 1063–1074.
Murawski, S.A., Hollander, D.J., Gilbert, S., Gracia, A., 2020. Deepwater Oil and Gas Production in the Gulf of Mexico and Related Global Trends. In: Murawski, S. (Ed.), Scenarios and Responses to Future Deep Oil Spills. Springer, Cham.
Murtagh, F., Legendre, P., 2014. Ward's hierarchical agglomerative clustering method: which algorithms implement Ward's criterion? J. Classif. 31 (3), 274–295.
Olivar, M.P., Bode, A., López-Pérez, C., Hulley, P.A., Hernández-León, S., 2019. Trophic position of lanternfishes (Pisces: Myctophidae) of the tropical and equatorial Atlantic estimated using stable isotopes. ICES J. Mar. Sci. 76 (3), 649–661.
Pakhomov, E.A., Henschke, N., Hunt, B.P., Stowasser, G., Cherel, Y., 2019. Utility of salps as a baseline proxy for food web studies. J. Plankton Res. 41 (1), 3–11.
Palomares, M.L.D. and D. Pauly. Editors. 2021. SeaLifeBase.
Parker, P.L., Anderson, R.K., Lawrence, A., 1989. A δ 13 C and δ 15 N tracer study of nutrition in aquaculture: Penaeus vannamei in a pond growout system. In: Stable Isotopes in Ecological Research. Springer, New York, pp. 288–303.
Parzanini, C., Parrish, C.C., Hamel, J.F., Mercier, A., 2017. Trophic ecology of a deep-sea fish assemblage in the Northwest Atlantic. Mar. Biol. 164 (10), 206.
Passarella, K.C., Hopkins, T.L., 1991. Species composition and food habits of the micronektonic cephalopod assemblage in the eastern Gulf of Mexico. Bull. Mar. Sci. 49 (1–2), 638–659.
Pauly, D., Trites, A.W., Capuli, E., Christensen, V., 1998. Diet composition and trophic levels of marine mammals. ICES J. Mar. Sci. 55 (3), 467–481.
Pearre Jr., S., 2003. Eat and run? The hunger/satiation hypothesis in vertical migration: history, evidence and consequences. Biol. Rev. 78 (1), 1–79.
Peterson, B.J., Fry, B., 1987. Stable isotopes in ecosystem studies. Annu. Rev. Ecol. Syst. 18 (1), 293–320.
Pinnegar, J.K., Polunin, N.V.C., 1999. Differential fractionation of δ13C and δ15N among fish tissues: implications for the study of trophic interactions. Funct. Ecol. 13 (2), 225–231.
Post, D.M., 2002. Using stable isotopes to estimate trophic position: models, methods, and assumptions. Ecology 83 (3), 703–718.
Post, D.M., Layman, C.A., Arrington, D.A., Takimoto, G., Quattrochi, J., Montana, C.G., 2007. Getting to the fat of the matter: models, methods and assumptions for dealing with lipids in stable isotope analyses. Oecologia 152 (1), 179–189.
Queen, J.P., Quinn, G.P., Keough, M.J., 2002. Experimental design and data analysis for biologists. Cambridge University Press.
Ramirez-Llodra, E., Tyler, P.A., Baker, M.C., Bergstad, O.A., Clark, M.R., Escobar, E., et al., 2011. Man and the last great wilderness: human impact on the deep sea. PLoS One 6 (8), e22588.
Richards, T.M., Gipson, E.E., Cook, A., Sutton, T.T., Wells, R.D., 2019. Trophic ecology of meso-and bathypelagic predatory fishes in the Gulf of Mexico. ICES J. Mar. Sci. 76 (3), 662–672.

Richards, T.M., Sutton, T.T., Wells, R.J., 2020. Trophic structure and sources of variation influencing the stable isotope signatures of meso-and bathypelagic micronekton fishes. Front. Mar. Sci. 7, 876.
Romero-Romero, S., Molina-Ramírez, A., Höfer, J., Acuña, J.L., 2016. Body size-based trophic structure of a deep marine ecosystem. Ecology 97 (1), 171–181.
Romero-Romero, S., Choy, C.A., Hannides, C.C., Popp, B.N., Drazen, J.C., 2019. Differences in the trophic ecology of micronekton driven by diel vertical migration. Limnol. Oceanogr. 64 (4), 1473–1483.
Rooker, J.R., Kitchens, L.L., Dance, M.A., Wells, R.D., Falterman, B., Cornic, M., 2013. Spatial, temporal, and habitat-related variation in abundance of pelagic fishes in the Gulf of Mexico: potential implications of the Deepwater Horizon oil spill. PLoS One 8 (10), e76080.
Saba, G.K., Burd, A.B., Dunne, J.P., Hernández-León, S., Martin, A.H., Rose, K.A., Wilson, S.E., 2021. Toward a better understanding of fish-based contribution to ocean carbon flux. Limnol. Oceanogr. 66 (5), 1639–1664.
Sakano, H., Fujiwara, E., Nohara, S., Ueda, H., 2005. Estimation of nitrogen stable isotope turnover rate of Oncorhynchus nerka. Environ. Biol. Fishes 72 (1), 13–18.
Schlacher, T.A., Connolly, R.M., 2014. Effects of acid treatment on carbon and nitrogen stable isotope ratios in ecological samples: a review and synthesis. Methods Ecol. Evol. 5 (6), 541–550.
Sutton, T.T., Clark, M.R., Dunn, D.C., Halpin, P.N., Rogers, A.D., Guinotte, J., et al., 2017a. A global biogeographic classification of the mesopelagic zone. Deep Sea Res. Part I 126, 85–102.
Sutton, T.T., Hopkins, T.L., 1996a. Trophic ecology of the stomiid (Pisces: Stomiidae) fish assemblage of the eastern Gulf of Mexico: strategies, selectivity and impact of a top mesopelagic predator group. Mar. Biol. 127 (2), 179–192.
Sutton, T.T., Hopkins, T.L., 1996b. Species composition, abundance, and vertical distribution of the stomiid (Pisces: Stomiiformes) fish assemblage of the Gulf of Mexico. Bull. Mar. Sci. 59 (3), 530–542.
Sutton, T.T., Frank, T., Judkins, H., Romero, I.C., 2020. As Gulf Oil Extraction Goes Deeper, Who Is at Risk? Community Structure, Distribution, and Connectivity of the Deep-Pelagic Fauna. In: Murawski, S. (Ed.), Scenarios and Responses to Future Deep Oil Spills. Springer, Cham.
Sweeting, C.J., Barry, J., Barnes, C., Polunin, N.V.C., Jennings, S., 2007. Effects of body size and environment on diet-tissue δ15N fractionation in fishes. J. Exp. Mar. Biol. Ecol. 340 (1), 1–10.
Thurber, A.R., Sweetman, A.K., Narayanaswamy, B.E., Jones, D.O., Ingels, J., Hansman, R.L., 2014. Ecosystem function and services provided by the deep sea. Biogeosciences 11 (14), 3941–3963.
Trueman, C.N., Johnston, G., O'Hea, B., MacKenzie, K.M., 2014. Trophic interactions of fish communities at midwater depths enhance long-term carbon storage and benthic production on continental slopes. Proc. R. Soc. B Biol. Sci. 281 (1787), 20140669.
Valls, M., Olivar, M.P., de Puelles, M.F., Molí, B., Bernal, A., Sweeting, C.J., 2014. Trophic structure of mesopelagic fishes in the western Mediterranean based on stable isotopes of carbon and nitrogen. J. Mar. Syst. 138, 160–170.
Vanderklift, M.A., Ponsard, S., 2003. Sources of variation in consumer-diet δ 15 N enrichment: a meta-analysis. Oecologia 136, 169–182.
Vereshchaka, A.L., Lunina, A.A., Sutton, T., 2019. Assessing deep-pelagic shrimp biomass to 3000 m in The Atlantic Ocean and ramifications of upscaled global biomass. Sci. Rep. 9 (1), 5946.
von Harbou, L., Dubischar, C.D., Pakhomov, E.A., Hunt, B.P., Hagen, W., Bathmann, U. V., 2011. Salps in the Lazarev Sea, Southern Ocean: I. Feeding dynamics. *Mar. Biol.* 158 (9), 2009–2026.
Vukovich, F.M., Crissman, B.W., 1986. Aspects of warm rings in the Gulf of Mexico. J. Geophys. Res. Oceans 91 (C2), 2645–2660.
Wada, E., Mizutani, H., Minagawa, M., 1991. The use of stable isotopes for food web analysis. Crit. Rev. Food Sci. Nutr. 30 (4), 361–371.
Ward Jr, J.H., 1963. Hierarchical grouping to optimize an objective function. J. Am. Stat. Assoc. 58 (301), 236–244.
Webb, T.J., Berghe, E.V., O'Dor, R., 2010. Biodiversity's big wet secret: the global distribution of marine biological records reveals chronic under-exploration of the deep pelagic ocean. PLoS One 5 (8), e10223.
Wells, R.D., Rooker, J.R., Quigg, A., Wissel, B., 2017. Influence of mesoscale oceanographic features on pelagic food webs in the Gulf of Mexico. Mar. Biol. 164 (4), 92.
Winemiller, K.O., Polis, G.A., 1996. Food webs: what can they tell us about the world? Food Webs. Springer, Boston, MA.
Woodstock, M.S., Blanar, C.A., Sutton, T.T., 2020. Diet and parasites of a mesopelagic fish assemblage in the Gulf of Mexico. Mar. Biol. 167 (12), 1–9.
Young, J.W., Hunt, B.P., Cook, T.R., Llopiz, J.K., Hazen, E.L., Pethybridge, H.R., Choy, C. A., 2015. The trophodynamics of marine top predators: current knowledge, recent advances and challenges. Deep Sea Res. Part II 113, 170–187.
Zanden, M.J.V., Rasmussen, J.B., 2001. Variation in $\delta^{15}N$ and $\delta^{13}C$ trophic fractionation: implications for aquatic food web studies. Limnol. Oceanogr. 46 (8), 2061–2066.